Received: 4 June 2024 | Revised: 4 July 2024 | Accepted: 8 July 2024

DOI: 10.1002/ar.25545

RESEARCH ARTICLE

The Anatomical Record WILEY

A juvenile pleurosaurid (Lepidosauria: Rhynchocephalia) from the Tithonian of the Mörnsheim Formation, Germany

Victor Beccari[1,2] | **Andrea Villa**[3] | **Marc E. H. Jones**[4,5] | **Gabriel S. Ferreira**[6,7] | **Frank Glaw**[8,9] | **Oliver W. M. Rauhut**[1,2,9]

[1]SNSB-Bayerische Staatssammlung für Paläontologie und Geologie, Munich, Germany

[2]Department of Earth and Environmental Sciences, Ludwig-Maximilians-Universität, Munich, Germany

[3]Institut Català de Paleontologia Miquel Crusafont (ICP-CERCA), Edifici ICTA-ICP, Barcelona, Spain

[4]Fossil Reptiles, Amphibians and Birds Section, Science Group, Natural History Museum, London, UK

[5]Research Department of Cell and Developmental Biology, Anatomy Building, UCL, University College London, London, UK

[6]Senckenberg Centre for Human Evolution and Palaeoenvironment at the University of Tübingen, Tübingen, Germany

[7]Fachbereich Geowissenschaften, Eberhard Karls Universität Tübingen, Tübingen, Germany

[8]SNSB-Zoologische Staatssammlung, Munich, Germany

[9]GeoBioCenter, Ludwig-Maximilians-Universität, Munich, Germany

Correspondence
Victor Beccari, SNSB-Bayerische Staatssammlung für Paläontologie und Geologie, Munich, Germany.
Email: victor.beccari@gmail.com

Funding information
DFG (10.13039/501100001659 – Deutsche Forschungsgemeinschaft), Grant/Award Number: RA 1012/28-1; Alexander von Humboldt Foundation; Secretaria d'Universitats i Recerca of the Departament de Recerca i Universitats, Generalitat de Catalunya, Grant/Award Number: 2021 BP 00038; CERCA Programme/Generalitat de Catalunya; Agència de Gestió d'Ajuts Universitaris i de Recerca of the Generalitat de Catalunya, Grant/Award Number: 2021 SGR 00620

Abstract

Late Jurassic rhynchocephalians from the Solnhofen Archipelago have been known for almost two centuries. The number of specimens and taxa is constantly increasing, but little is known about the ontogeny of these animals. The well-documented marine taxon *Pleurosaurus* is one of such cases. With over 15 described (and many more undescribed) specimens, there were no unambiguous juveniles so far. Some authors have argued that *Acrosaurus*, another common component of the Solnhofen Archipelago herpetofauna, might represent an early ontogenetic stage of *Pleurosaurus*, but the lack of proper descriptions for this taxon makes this assignment tentative, at best. Here, we describe the first unambiguous post-hatchling juvenile of *Pleurosaurus* and tentatively attribute it to *Pleurosaurus* cf. *P. ginsburgi*. The new specimen comes from the Lower Tithonian of the Mörnsheim Formation, Germany. This specimen is small, disarticulated, and incomplete, but preserves several of its craniomandibular bones and presacral vertebrae. It shares with *Pleurosaurus* a set of diagnostic features, such as an elongated and triangular skull, a low anterior flange in its dentition, and an elongated axial skeleton. It can be identified as a juvenile due to the presence of an unworn dentition, well-spaced posteriormost dentary teeth, a large gap between the last teeth and the coronoid process of the dentary, and poorly ossified vertebrae with unfused neural arches. *Acrosaurus* shares many anatomical features with both this specimen and *Pleurosaurus*,

which could indicate that the two genera are indeed synonyms. The early ontogenetic stage inferred for the new *Pleurosaurus* specimen argues for an even earlier ontogenetic placement for specimens referred to *Acrosaurus*, the latter possibly pertaining to hatchlings.

KEYWORDS

Jurassic, Mesozoic, Pleurosauridae, *Pleurosaurus*, Sphenodontia

1 | INTRODUCTION

Rhynchocephalians, today represented by a single species, *Sphenodon punctatus* (Gray, 1842) (see Hay et al., 2010), were highly diverse and common during the Mesozoic, especially in Europe, North and South America (e.g., Apesteguía, 2016; Chambi-Trowell et al., 2021; DeMar et al., 2022; Evans et al., 2001; Herrera-Flores et al., 2017; Hsiou et al., 2019; Jones, 2008, 2009; Rauhut et al., 2012; Simões et al., 2022). The Late Jurassic outcrops of the Solnhofen Archipelago, Germany, have yielded well-preserved, relatively complete specimens that have been known for almost two centuries (Goldfuss, 1831; Von Meyer, 1831; Von Meyer, 1854). These specimens have been assigned to up to 10 different genera: *Acrosaurus* Von Meyer, 1854, *Homoeosaurus* Von Meyer, 1847, *Kallimodon* Cocude-Michel, 1963, *Leptosaurus* Fitzinger, 1840, *Oenosaurus* Rauhut et al., 2012, *Pleurosaurus* Von Meyer, 1831, *Piocormus* Wagner, 1852, *Sapheosaurus* Von Meyer, 1850, *Sphenofontis* Villa et al., 2021, and *Vadasaurus* Bever & Norell, 2017. *Acrosaurus*, *Pleurosaurus*, and *Vadasaurus* are usually referred to the clade of pleurosaurids (e.g., Chambi-Trowell et al., 2021; Cocude-Michel, 1963; DeMar et al., 2022; Dupret, 2004; Reynoso, 2000).

Pleurosaurids are marine rhynchocephalians with a set of aquatic adaptations, i.e., slender, streamlined skull, elongated body, robust first metacarpal, unossified joint surfaces, and loss of autotomic septum in the caudal vertebrae (Bever & Norell, 2017; Carroll & Wild, 1994; Dupret, 2004; Jones, 2008; Klein & Scheyer, 2017; Lee et al., 2016; Meloro & Jones, 2012). The clade Pleurosauridae Lydekker, 1880 was defined in multiple occasions (i.e., Chambi-Trowell et al., 2021; Dupret, 2004; Simões et al., 2020). As in most clades, these definitions were originally apomorphy-based (e.g., Dupret, 2004), but phylogenetic definitions of Pleurosauridae as a node-based clade have recently been proposed (Chambi-Trowell et al., 2021; Simões et al., 2020), which, however, vary in their specifiers. Only *Pleurosaurus goldfussi* Von Meyer, 1831 and *Palaeopleurosaurus posidoniae* Carroll, 1985 were consistently recovered with general consensus within the clade (Bever & Norell, 2017; Chambi-Trowell et al., 2021; DeMar et al., 2022; Dupret, 2004; Klein & Scheyer, 2017; Martínez et al., 2021; Romo de Vivar et al., 2020; Simões et al., 2020, 2022). Taxa that are recovered as pleurosaurids by some authors, but whose position should be tested further, include *Derasmosaurus pietrarojae* Barbera & Macuglia, 1988 (i.e., analyses by Simões et al., 2020, 2022), *Vadasaurus herzogi* Bever & Norell, 2017 (i.e., analyses by Chambi-Trowell et al., 2021, but not on the analyses by DeMar et al., 2022), and *Tingitana anoualae* Evans & Sigogneau-Russell, 1997 (i.e., analyses by Chambi-Trowell et al., 2021). Another taxon considered to be a pleurosaurid is *Acrosaurus frischmanni* Von Meyer, 1854. However, the validity of this taxon has been questioned, with the general consensus regarding it as a hatchling or juvenile *P. goldfussi* (Dupret, 2004; Fabre, 1974, 1981; Hoffstetter, 1955; Jones, 2008; Rothery, 2002, 2005). Nevertheless, a different opinion was indeed presented by other authors, even recently (e.g., Cocude-Michel, 1963; Tischlinger & Rauhut, 2015).

The genus *Pleurosaurus* is the most abundant rhynchocephalian in the Late Jurassic deposits of Canjuers and Cerin, France and the Solnhofen Archipelago, Germany (Bever & Norell, 2017; Carroll & Wild, 1994; Cocude-Michel, 1963; Dupret, 2004; Fabre, 1974, 1981; Fabre et al., 1982; Jones, 2008; Klein & Scheyer, 2017; Rauhut et al., 2012; Rauhut & López-Arbarello, 2016; Villa et al., 2021; Von Meyer, 1831; Watson, 1914). The genus is defined as a pleurosaurid with an elongated, triangular skull, a recurved premaxilla, absence of postfrontal, low anterior flange on the teeth, reduced forelimbs, unossified limb bone epiphyses, absence of sigmoidal flexure in their stylopods, mediolaterally narrow tails with no autotomic septa, and reduced carpals (Dupret, 2004). There are currently two species in this genus, *P. goldfussi* and *Pleurosaurus ginsburgi* Fabre, 1974. Specific distinction is based on differences in the number of presacral vertebrae (50 and 57, respectively), skull versus appendicular bone proportions, and the development of the pelvis, being more developed, that is, with a more robust dorsal process of the ilium, in *P. goldfussi* (Dupret, 2004). Previous studies generally accept both species of *Pleurosaurus* as distinct (Bever & Norell, 2017; Dupret, 2004; Fabre, 1974, 1981; Reynoso, 2000; Simões et al., 2020, 2022; Villa et al., 2021 but see Rothery, 2005), although a more detailed study of a higher number of specimens would be necessary to firmly establish this distinction.

Although extensive research has been done on *Pleurosaurus*, with over 15 published specimens

(Cocude-Michel, 1963; Dupret, 2004; Fabre, 1974, 1981), no unambiguous juvenile specimen of this taxon has been described so far (but see Dames, 1896; Von Huene, 1952). The lack of *Pleurosaurus* juvenile specimens bears important implications on our understanding of their ontogeny and the validity of *Acrosaurus*. Here, we describe the first occurrence of an early juvenile rhynchocephalian that is securely referable to *Pleurosaurus*, coming from the Tithonian deposits of the Mörnsheim Formation, Solnhofen Archipelago, Germany. We also discuss the importance of this specimen in understanding pleurosaurid ontogeny and the distribution of Pleurosauridae during the Jurassic.

2 | GEOLOGICAL SETTING

The juvenile specimen described here comes from the Mörnsheim Formation close to Mühlheim, near Solnhofen, Bavaria, Germany. The Mörnsheim Formation is the uppermost unit of the Late Jurassic complex of Konservat Lagerstätten in southern Germany that are often collectively being referred to as "Solnhofen limestones." These "Solnhofen limestones" actually represent a series of formations within the upper part of the Late Jurassic Weißjura Group (Niebuhr & Pürner, 2014), which span two ammonite zones, from the Upper Kimmeridgian *Hybonoticeras beckeri* Zone to the Lower Tithonian *Hybonoticeras hybonotum* Zone (Mäuser, 2015; Schweigert, 2007). The exact formation names and correlations of the units representing the "Solnhofen limestones" differ from the western to the eastern outcrop areas. In the area west of Ingolstadt, in which the locality is found, the sequence starts with the Torleite Formation (Upper Kimmeridgian, Subeumela to Setatum ammonite subzone), followed by the Geisental Formation (Kimmeridgian-Tithonian boundary, Setatum to Riedense ammonite subzone), the Altmühltal Formation (Lower Tithonian, Riedense to Ruepellianus ammonite subzone), and finally capped by the Mörnsheim Formation (Lower Tithonian, Moernsheimensis ammonite subzone; see Mäuser, 2015; Niebuhr & Pürner, 2014). Although most of the famous fossils of the "Solnhofen limestones" come from the Altmühltal Formation, these other formations, and a more eastern equivalent of the Altmühltal Formation, the Painten Formation, are also very fossiliferous, so that in the more recent literature, the setting of the "Solnhofen limestones" has usually been referred to as the "Solnhofen Archipelago" (e.g., Rauhut et al., 2017; Röper, 2005).

The fine-grained calcareous sediments of the Solnhofen Archipelago accumulated in a shallow marine setting at the northern rim of the Tethys, in several, rather small-scaled depocenters (the so-called "Wannen") delimited by sponge and coral reefs (see Meyer & Schmidt-Kaler, 1989; Viohl, 2015). The locality at the Schaudiberg, close to Mühlheim, lies within the Solnhofen/Langenaltheim Basin. In this basin, the Solnhofen Member of the Altmühltal Formation is overlain by the Mörnsheim Formation, being separated from the latter by the "Hangende Krumme Lage," a slumping horizon in the uppermost part of the Altmühltal Formation. Whereas the latter unit is characterized by an alternation of extremely pure and fine-grained limestones ("Flinze," more than 96% carbonate content) and more marly limestones ("Fäulen," carbonate content >85%; see Munnecke et al., 2008), the Mühlheim Member of the Mörnsheim Formation, which is exposed in the vicinity of Mühlheim, consists of silicious limestones with abundant fossil debris in at least parts of the profile (see Heyng et al., 2015; Niebuhr & Pürner, 2014). At the Schaudiberg, the lower part of the Mörnsheim Formation is exposed, with an estimated total thickness of about 50 m (Heyng et al., 2015). Two quarries are present at the Schaudiberg, the Old Schöpfel quarry and a visitor quarry. The boundary between the Altmühltal Formation and the Mörnsheim Formation was originally exposed in the Old Schöpfel Quarry, but the lowermost few meters of the latter unit are currently covered. At the moment, approximately 8 m of the lowermost section of the Formation are exposed in the quarry, dominated by silicified laminated and massive limestones in the lower part and more laminated limestones, marly limestones and occasional clays in the higher part of the section. The specimen described here comes from this upper part of the section within the Old Schöpfel Quarry, from a layer that has also yielded several specimens of adult *Pleurosaurus* (U. Leonhardt, pers. comm. to OWMR, 2024).

3 | MATERIALS AND METHODS

3.1 | Studied specimen and comparative material

This study focuses on SNSB-BSPG 2018 I 179 (Figure 1), a small rhynchocephalian specimen housed in the collections of the Bayerische Staatssammlung für Paläontologie und Geologie (SNSB-BSPG), Munich. It is a yet unreported and undescribed specimen from Schaudiberg, Mühlheim, Germany. The specimen is publicly available. The osteological description in this manuscript follows the nomenclature and orientation proposed by Evans (2008) and Jones et al. (2011) for the skull, Hoffstetter and Gasc (1969) for the axial skeleton, and Russell and Bauer (2008) for the appendicular skeleton. The ontogenetic status of SNSB-BSPG 2018 I 179 is evaluated based on information previously published for ontogeny in rhynchocephalians (i.e., Evans, 2008; Hoffstetter & Gasc, 1969; Jones, 2008; Simões et al., 2022). In addition, the studied specimen was

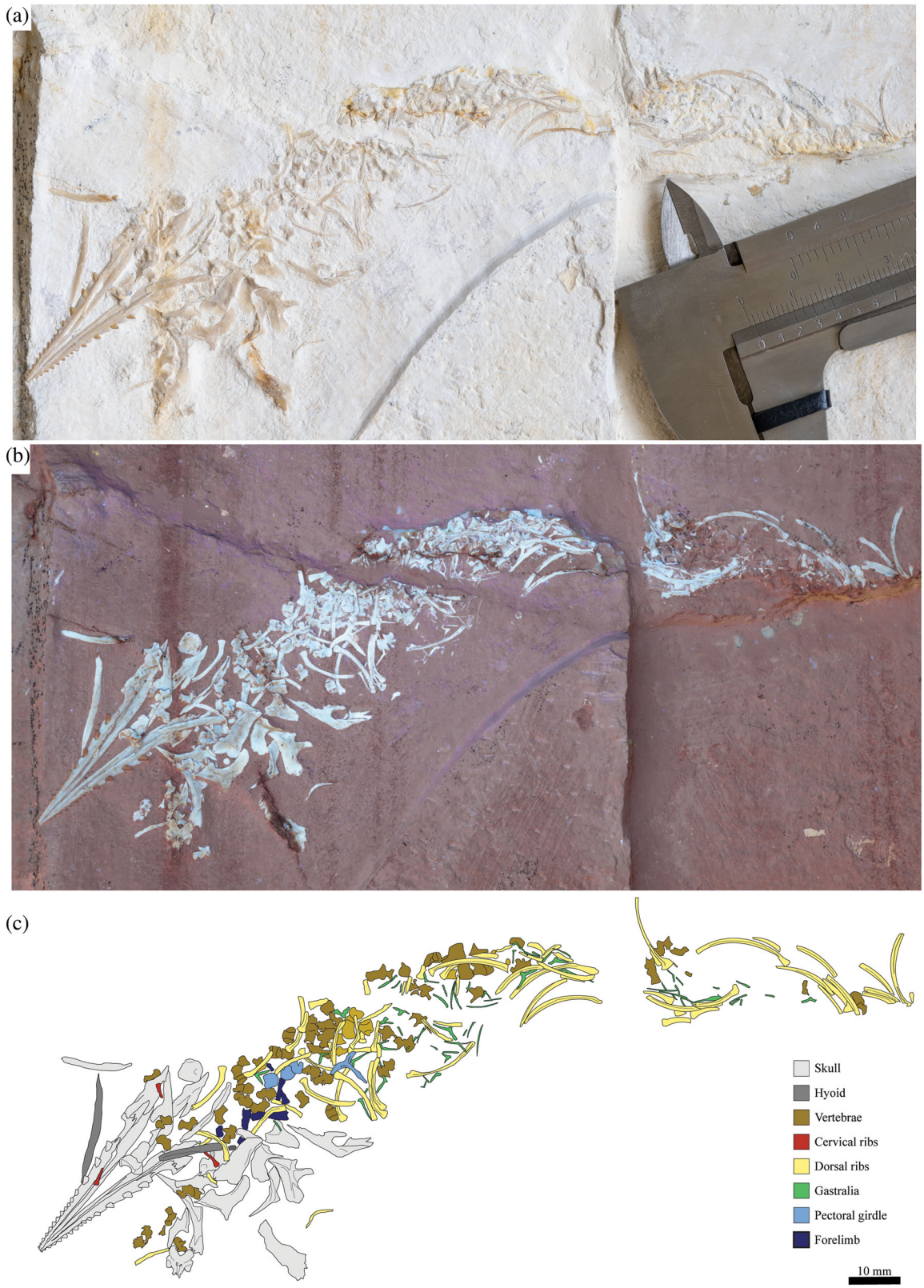

FIGURE 1 *Pleurosaurus* cf. *P. ginsburgi* SNSB-BSPG 2018 I 179. (a) Photograph in standard light, (b) photograph under UV light, and (c) interpretative illustration of the specimen.

compared with specimens of the extant *S. punctatus*, of different ontogenetic categories, as well as fossil rhynchocephalians (VB, personal observations). Fossils used for comparisons include taxa from the Late Jurassic of the Solnhofen Archipelago (i.e., *Acrosaurus*, *Homoeosaurus*, *Kallimodon*, *Leptosaurus*, *Oenosaurus*, *Pleurosaurus*,

Sapheosaurus, *Sphenofontis*, and *Vadasaurus*), as well as pleurosaurids and possible pleurosaurids from other localities (i.e., *Palaeopleurosaurus* Carroll, 1985, *Tingitana* Evans & Sigogneau-Russell, 1997, and *Derasmosaurus* Barbera & Macuglia, 1988).

3.2 | Photographs and figures

The specimen was photographed using a mirrorless OM-1 (OM Digital Solutions, Shinjuku, Tokyo, Japan) camera with an Olympus M.Zuiko Digital ED 60 mm F2.8 Macro lens. For the UV photography, we used the Alonefire SV003 10W UV-lamp—365 nm (Shenzhen Shiwang Technology Co., Guangdong, China). No filters were used to acquire the pictures. All photographs were digitally edited in Adobe Lightroom Classic 2024 (Adobe, San Jose, CA, USA). The figures were created using Adobe Illustrator 2024.

3.3 | CT-scan and image segmentation

The specimen SNSB-BSPG 2018 I 179 was scanned at the 3D Imaging Lab of the University of Tübingen using a Nikon XT H 320 with a tungsten reflection target with maximum voltage of 225 kV. The tomographic dataset was acquired focusing on the skull region with 215 kV and 147 µA, using a copper filter of 1.5 mm thickness and a voxel size of 31.74 µm. We took 4476 projections holding four frames per projection at 708 ms, 0.057051 mm voxel size (data available at MorphoSource: ark:/87602/m4/629350). The data derived from the CT-scan was segmented (Image Segmentation) using the software Avizo v9.2 (Thermo Fisher Scientific, MA, USA). The segmentation was done manually, using the brush function and interpolation. The resulting meshes were then exported in wavefront (.obj) file format and treated in Blender v4.0 (Blender Foundation, Amsterdam, Netherlands). The meshes were cleaned to remove floating geometries, then smoothed using the Smooth modifier (factor = 1, repeat = 5) for rendering. The measurements were taken digitally in Blender.

TABLE 1 Measurements of *Pleurosaurus* cf. *P. ginsburgi* SNSB-BSPG 2018 I 179. All measurements are in mm.

Dentary length	36.74 (l)
Mandible length	43.45 (l[a]); 43.24 (r)
Mandibular rami divergence angle	15°
Dentary posterior height, before coronoid process	3.61 (l)
Dentary symphysial height	0.61 (l)
Tooth count	15 (l and r)
Ceratobranchial length	16.3; 16.8
Ceratobranchial diameter at midlength	1.17; 1.17
Frontal length	11.61 (l)
Parietal length	12.58 (l)
Postorbital length between anterior and posterior processes	11.88 (l[b]); 12.16 (r)
Squamosal length between anterior and posterior processes	11.35 (l); 11.88 (r)
Pterygoid length	11.08 (l); 11.01 (r)
Humerus length	7.26 (r)
Humerus length (HL)/skull length (SL)	0.17 (r)
Radius length	4.92 (r[a])

Abbreviations: L, left; r, right.
[a]Measurement taken on reconstructed specimen.
[b]Broken or poorly preserved element.

3.4 | Institutional abbreviations

AMNH FARB, American Museum of Natural History, Paleontology: Fossil Amphibians, Reptiles, and Birds, New York, USA; DM, Dinosaur National Monument, Vernal, UT, USA; MCM and MNHN, Muséum national d'Histoire naturelle, Paris, France; MPN, Museo di Paleontologia, Naples, Italy; NHMLA, Natural History Museum of Los Angeles County, Los Angeles, CA, USA; NHMUK, Natural History Museum London, Collection Specimen, London, England; QMUL QMBC, Queen Mary University of London, Queen Mary Biology Collection, London, England; SMF, Senckenberg Naturmuseum, Frankfurt, Germany; SMNS, Staatliches Museum für Naturkunde Stuttgart; SNSB-BSPG, Bayerische Staatssammlung für Paläontologie und Geologie, Munich, Germany; TM, Tylers Museum, Haarlem, Netherlands; SNSB-ZSM, Zoologische Staatssammlung München Sammlungen, Bavarian State Collection of Zoology Collections, Munich, Germany. YB, Yale Peabody Museum, New Haven, CT, USA.

4 | SYSTEMATIC PALEONTOLOGY

Lepidosauria Haeckel, 1866.
Rhynchocephalia Günther, 1867.
Sphenodontia Williston, 1925.
Pleurosauridae Lydekker, 1880.
Pleurosaurus Von Meyer, 1831.
Pleurosaurus ginsburgi Fabre, 1974.
Pleurosaurus cf. *P. ginsburgi*.

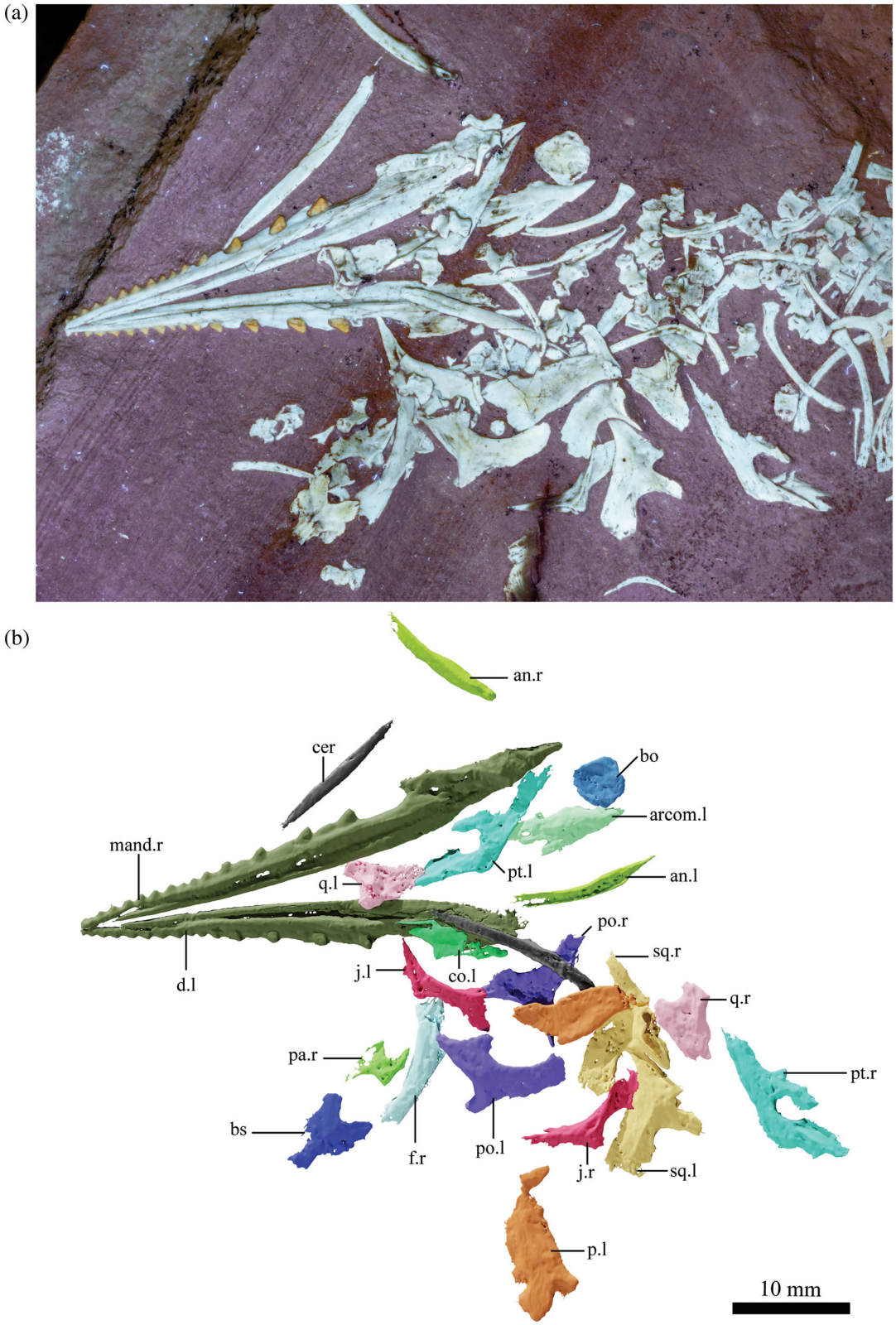

FIGURE 2 Skull of *Pleurosaurus* cf. *P. ginsburgi* SNSB-BSPG 2018 I 179. (a) Photograph under UV light and (b) 3D representation of the skull bones of SNSB-BSPG 2018 I 179. an, angular; arcom, articular complex; bo, basioccipital; bs, basisphenoid; cer, ceratobranchial; co, coronoid; d, dentary; f, frontal; j, jugal; mand, mandibular ramus; p, parietal; pa, palatine; po, postorbital; pt, pterygoid; q, quadrate; sq, squamosal; l, left; r, right.

Specimen remarks: SNSB-BSPG 2018 I 179 can be assigned to the genus *Pleurosaurus* due to the elongated, triangular skull, absence of separated postfrontal and postorbital, presence of low anterior flanges in the dentary teeth, and elongated presacral series. It can tentatively be assigned to *P. ginsburgi* due to humerus length to skull length (SL) proportions being less than 0.2.

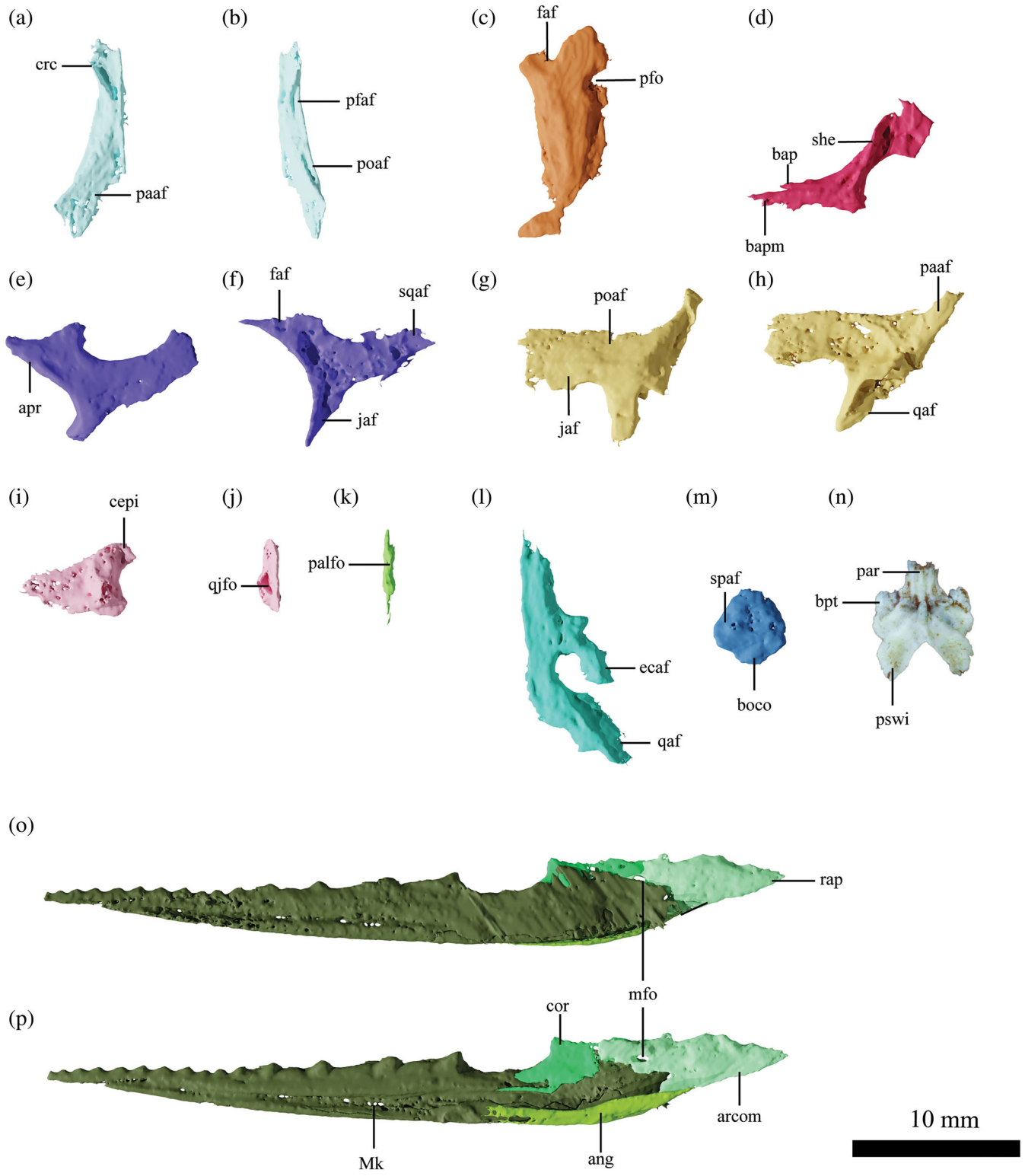

FIGURE 3 Legend on next page.

5 | DESCRIPTION

SNSB-BSPG 2018 I 179 (Figure 1) is small (Table 1), disarticulated, and incomplete, with most of the posterior half of the animal missing. The upper jaws, the posterior region of the axial skeleton, and most of the appendicular skeleton are missing. The cranial bones are disarticulated, except for some bones of the lower jaws. The axial skeleton is disarticulated, displaced, and poorly preserved. Its bones overlap each other.

5.1 | Skull

5.1.1 | General features

The skull bones are disarticulated and displaced, but overall, well preserved (Figures 2 and 3). Identifiable cranial elements include: right frontal, both parietals, both jugals, both postorbitals, both squamosals, both quadrates, a fragment of the right palatine, both pterygoids, sphenoid, and the basioccipital. Premaxillae, maxillae, prefrontals, vomers, ectopterygoids, as well as most of the braincase elements are either missing or cannot be identified. Due to the disarticulation of the bones, it is not possible to estimate the size and shape of the skull openings. However, SL would be around 38–40 mm long, estimated based on the lower jaw total length (see Section 3.7).

5.1.2 | Frontal

The right frontal is preserved and exposed in dorsal view. In the same view, it is generally trapezoidal, widening posteriorly, and longer than wide, with a concave lateral margin, partially due to a marked lateral expansion of the bone posterior to the orbit. The interfrontal articulation margin is straight. Anteriorly, the anterior end of the frontal widens but is incomplete, and ventrally bears a large medial the facet for the nasal and a smaller lateral facet for the prefrontal (similar but not identical to *Sphenodon* Gray, 1831: Jones et al., 2011). Anteriorly, the nasal and prefrontal facets appear contiguous (Figure 3a). The articular facet of the prefrontal continues posteriorly along the anterolateral margin of the frontal. The postorbital slots into the bone at the posterolateral margin (Figure 3b). The facets for the prefrontal and postorbitofrontal are separated such that the frontal would thus participate rather extensively in the dorsal margin of the orbit. The posterior process of the frontal is convex laterally and concave medially. It expands posteriorly and limits the contact between parietal and postorbital (at least in dorsal view). The frontal does not participate in the parietal foramen. In ventral view, the frontal has a marked, curved crista cranii that delimits the orbit and almost extends to the interfrontal suture medially in the narrowest part of the bone. Anteriorly, an anteriorly widening depressed facet is present between the crista cranii and the interfrontal suture (Figure 3a).

5.1.3 | Parietal

Both parietals are preserved, displaced from each other. The left parietal is exposed in dorsolateral view, and the right one in ventral view. As preserved, the parietal is rectangular, wider anteriorly than posteriorly, although this is partially due to the flattening of the originally three-dimensional bone. The parietal foramen is completely encircled by the parietals. The foramen is circular (Figure 3c). Lateral to the foramen, a slightly raised step marks the transition from the dorsal surface of the parietal to its dorsolateral surface that would have formed the medial wall of the supratemporal fenestra but has been flattened into almost the same plane as the dorsal surface by compression. The dorsal surface gradually narrows from the anterior end of the supratemporal fenestra posteriorly, so that only a narrow sagittal crest seems to have been present toward the posterior end of the parietal, where the bone is damaged, however. Anterolaterally, a marked,

FIGURE 3 3D representation of selected bones of *Pleurosaurus* cf. *P. ginsburgi* SNSB-BSPG 2018 I 179. (a) Mirrored right frontal in ventral view, (b) mirrored right frontal in lateral view, (c) left parietal in dorsal view, (d) right jugal in medial view, (e) left postorbital in lateral view, (f) right postorbital in medial view, (g) left squamosal in lateral view, (h) right squamosal in medial view, (i) mirrored right quadrate in lateral view, (j) mirrored right quadrate in posterior view, (k) right palatine in lateral view, (l) right pterygoid in ventral view, (m) basioccipital in ventral view, (n) UV-photograph of sphenoid in ventral view, (o) reconstructed left mandible in lateral view, and (p) mirrored reconstructed left mandible in medial view. ang, angular; apr, ascending process; arcom, articular complex; bapl, bifid anterior process, lateral process; bapm, bifid anterior process, medial process; boco, basioccipital condyle; bpt, basipterygoid process; cepi, central pillar; cor, coronoid process; crc, crista cranii; ecaf, ectopterygoid articular facet; faf, frontal articular facet; jaf, jugal articular facet; mfo, mandibular foramen; Mk, Meckelian fossa; paaf, parietal articular facet; par, parasphenoid; palfo, palatine foramen; pfaf, prefrontal articular facet; pfo, parietal foramen; poaf, postorbital articular facet; pswi, parasphenoid wing; qaf, quadrate articular facet; qjfo, quadratojugal foramen; rap, retroarticular process; she, shelf; spaf, sphenoid articular facet; sqaf, squamosal articular facet.

depressed facet is present on the dorsal surface of the parietal just anterior to the rim of the supratemporal fenestra (Figure 3c). This facet is semioval, with a thin flange extending anteromedially, and was overlain by the posterolateral end of the frontal medially and the posteromedial end of the postorbital laterally. The posterior end of the parietal curves posterolaterally to form the squamosal process (Figure 3c). The posteromedial margin of this process is straight, going from anteromedial to posterolateral.

5.1.4 | Jugal

Both jugals are preserved, the left one in lateral view and the right one in medial view. The jugal has two well-developed processes, an anterior and an ascending (dorsal or posterodorsal in Evans, 2008) processes (Figure 3d), but it lacks a well-developed caudal quadratojugal process. The anterior process is mediolaterally widened and bifid (Figure 3d), with a lateral and medial expansions tapering anteriorly. The medial expansion is slightly longer than the lateral one. The lateral surface exhibits a recess which corresponds to the facet for the maxilla. This mediolaterally widened anterior process would have overlain the posterior part of the maxilla and formed the posteroventral border of the orbit. The ascending processes of the jugal is broken at the distal end in both the left and right bones. The ascending process is constricted at its base and expands anteroposteriorly at its distal half. The anteromedial margin of this process shows a small groove for the articulation with the ventral process of the postorbital. This articulation facet forms a medial shelf in the jugal. The anterior process of the squamosal slots into the posterior margin of this shelf. The jugal contacts the anterior process of the squamosal medially at the expanded half of the ascending process. A small "bump" is present at the posteroventral margin of the jugal. This is here interpreted as an incipient quadratojugal process, which does not extend posteriorly.

5.1.5 | Postorbital

The left postorbital is preserved in lateral view, and the right postorbital is preserved in ventromedial view, obscured by other bones (i.e., a ceratobranchial of the hyoid, and the left parietal). Von Huene (1952) and subsequent authors (e.g., Carroll & Wild, 1994) argued that the postfrontal is fused without visible suture with the postorbital in *Pleurosaurus*, but the absence of a separate ossification or even a visible suture even in this juvenile specimen might indicate that the former bone is simply absent. Alternatively, the postfrontal might be fused to the frontal, as the latter seems to be more laterally expanded behind the orbit than it is the case in other rhynchocephalians and extends posterolaterally to almost the anterior margin of the supratemporal fenestra. However, again, no suture is visible either on the specimen directly or in the CT data, so nothing can be said about a possible fusion of the postfrontal with certainty. Therefore, we prefer to call the bone dealt with here as postorbital. Thus, the postorbital is a triradiated bone that articulates to the frontal and parietal dorsomedially, the jugal ventrally, and the squamosal posterodorsally (Figure 3e,f). The anteromedial (lateral in Jones et al., 2011) process is wide, expanding both antero- and posteriorly toward its medial end. The shortest process of the postorbital is the ventral one, which is triangular in outline and rapidly tapers ventrally. Together with the anterior process, it forms the posterodorsal margin of the orbit. The ventral process articulates posteroventrally with the jugal for its entire length. The posterior process is the longest branch of the postorbital. Together with the posterior margin of the anterior process, it forms the anterolateral margin of the upper temporal fenestra. This process is tongue-shaped and contacts the squamosal medially and posteriorly and the jugal ventrally. It has a rounded end.

5.1.6 | Squamosal

Both squamosals are preserved, the left one in lateral view and the right one in medial view. This bone is robust and composed of an anterior process that contacts the postorbital dorsolaterally and the jugal ventrolaterally, a bifid ventral process that locks the quadrate head, and a slender posterior medial process that contacts the parietal medially (Figure 3g,h). The anterior process is the largest of the three and is dorsoventrally deep. The articular facets for the postorbital and jugal are separated by a well-marked longitudinal ridge. The facet for the postorbital is a flat recess and extends to a point above where the jaw articulation would be and ends in a round margin. It extends considerably further posteriorly than the jugal articular facet, which is triangular and ends in a sharp edge. The dorsal margin of the anterior process is straight and forms the lateral margin of the upper temporal fenestra. The bifid ventral process includes the cotyle for the quadrate head and articulates with it medially. This articulation is deep. Together with the ventral margin of the anterior process, the ventral process bounds the posterodorsal margin of the ventrally open lower temporal fenestra. The posterior process of the squamosal is directed medially and tapers distally. The posterior margin of this process is straight.

5.1.7 | Quadrate

The left quadrate is preserved and exposed in medial view, and the right quadrate is preserved in lateral view. The quadrate is a dorsoventrally short bone that widens considerably toward the ventral articular end. It has a well-developed medial lamina and a slightly curved central pillar (Figure 3i). The medial lamina is a thin sheet of bone, rectangular, slightly longer than tall, and would articulate with the pterygoid. It is not clear if the squamosal would contact this lamina, as in *Sphenodon* (Evans, 2008; Jones et al., 2011). The central pillar shows a deep sulcus for the articulation to the squamosal at the dorsolateral surface, and a slightly shallower ventral sulcus for the articulation with the quadratojugal. The posterior margin of the quadrate pillar is concave and pierced by the quadratojugal foramen (Figure 3j). This foramen does not open anteriorly, as is the case for *Sphenodon* (Evans, 2008; Jones et al., 2011). The quadrate head is rounded. The mandibular articulation is composed by two asymmetrical condyles, with the medial condyle being larger and projecting further ventrally than the lateral one. The two condyles are separated by a deep and wide concavity and would have flanked a longitudinal ridge on the articular medially and laterally, probably indicating a propalinal jaw movement, as in the recent *Sphenodon*.

5.1.8 | Palatine

A fragment of the anterior region of the right palatine is preserved in this specimen. This fragment represents the lateral process of the palatine that articulates to the prefrontal and maxilla. It is concave anteriorly and posteriorly in dorsal view. The articular facet to the maxilla and prefrontal is straight in dorsal view. A small foramen opens medial to the contact of the palatine to the maxilla (Figure 3k). The ventral view is not exposed.

5.1.9 | Pterygoid

Both pterygoids are preserved and exposed in ventral view (Figures 2 and 3l). The pterygoid is triradiate, with a long and slender anterior process that articulates with the palatine, a lateral pterygoid flange that articulates with the ectopterygoid, and a dorsoventrally deep posterior process that articulates with the medial lamina of the quadrate. The articulation surface for the basipterygoid processes of the sphenoid is not visible and might not be preserved. The palatine process is long, slender and triangular in ventral view and tapers to a point at its anterior end. The interpterygoid articulation (medial margin) is straight and extends from the anterior tip of the palatine process to the base of the quadrate process. At the mid-length of the pterygoid, the pterygoid flange expands posterolaterally. The process is short and extends further laterally at its slender posterior flange. The ectopterygoid facet is present as an anteromedially to posterolaterally directed groove on the lateral surface of the pterygoid flange. The posterior margin of the flange is curved. The quadrate process diverges posterolaterally from the main axis of the pterygoid at an almost 45° angle. The process was originally probably twisted at a more pronounced angle of up to 90° toward the anterior and lateral processes but has partially been flattened into the same plane by compaction. It has a deep dorsal lamina that contacts the quadrate medial lamina throughout its length.

5.1.10 | Basioccipital

The basioccipital is preserved in dorsal view close to the disarticulated left surangular. This bone is subcircular to diamond-shaped in dorsal view, and wider than long, and has a slightly concave dorsal surface. The occipital condyle is anteroposteriorly short, not offset from the body of the occipital by a marked neck and has a transversely semicircular articular facet. The ventral surface is marked laterally by the shallow sphenoid articular facet, which is oriented from anteromedially to posterolaterally (Figure 3m).

5.1.11 | Sphenoid

The sphenoid is preserved in ventral view. It is as wide as long, with a deep posterior notch marked laterally by short and wide parasphenoid wings (Figure 3n). The basipterygoid processes are ovoid, very short and slightly anteroventrally expanded. They are bound by a curved depression posteromedially that separates the processes from the parasphenoid wings, and separated by the trabeculae cranii, which are short and robust, anteriorly. Posterior to the base of the trabeculae, two elongate foramina mark the openings of the vidian canals.

5.2 | Mandible

5.2.1 | General features

The mandibles are the best-preserved portion of the skull of SNSB-BSPG 2018 I 179 (Figure 2). Both left and right

rami are in contact and most of the individual bones are still in articulation (Figure 3o,p), except for both angulars and the left articular complex (fused surangular–articular–prearticular). Both mandibular rami are slightly tilted laterally, so that they are exposed in medial view. The right mandible is the best preserved and is 43.24 mm long, measured from the anterior tip of the dentary to the posterior tip of the retroarticular process. The mandible is slender, and both dorsal and ventral margins are almost straight for most of their length. The Meckelian fossa is well marked, extending over the full length of the dentaries and is bound ventrally by the dorsal margin of the angular in its posterior part. The mandibular foramen is extremely reduced. The splenial is absent.

5.2.2 | Dentary

The dentaries are the largest bones in the mandible. They show the typical *Pleurosaurus* hyper-shallow condition (e.g., Bever & Norell, 2017; Dupret, 2004). The dentary is very slightly bowed, being gently convex ventrally. It tapers toward the anterior end and the symphysial end is narrow. The mandibular symphysis lies anteromedially and is extremely reduced. As preserved, the angle between the dentaries is 15°. The first tooth lies almost at the anterior tip of the dentary. The dentaries lack the ventrally projected mentonian process (sensu Simões et al., 2022; "chin" in Villa et al., 2021) that is otherwise typical for rhynchocephalian dentaries. The Meckelian fossa tapers anteriorly and closes at the level of the third tooth. The fossa becomes gradually wider posteriorly. The coronoid process is placed after a large gap distal to the last dentary tooth. It is obscured medially by the coronoid anteriorly and the surangular posteriorly. Ventrally, the posterior portion of the dentary is overlapped medially by the angular.

5.2.3 | Coronoid

Both left and right coronoids are broken dorsally. The coronoid has an elongated anterior process that flanks the dentary medially. This process appears bifid anteriorly, lodging the posterior end of the subdental table of the dentary. Its anterior margin is concave, forming a small anteriorly oriented hook. The dorsal margin is slightly convex. The posterior margin of the coronoid contacts the surangular with an intricate and complex outline.

5.2.4 | Angular

Both angulars are disarticulated and displaced, with the left one preserved in lateral view, and the right one in medial view. Each angulars are slender, anteroposteriorly elongate bones. The angular forms the posteroventral margin of the Meckelian fossa. It articulates with the dentary in its anterior half. Posteriorly, it covers the prearticular portion of the articular complex ventromedially, and even extends to the lateral surface of its articular portion (as evidenced by the presence of an articulation surface on the left articular complex; Figure 2). The dorsal margin of the angular is straight, whereas the ventral one is slightly convex. A longitudinal ridge crosses the posterior half of the angular medially.

5.2.5 | Articular complex (surangular–articular–prearticular)

The articular, prearticular, and surangular are fused into a single element, the articular complex. The left articular complex is displaced and preserved in lateral view (Figure 2), whereas the right one still articulates with the rest of the mandible and is exposed in medial view. The articular complex is long, contacting the coronoid anteromedially, the dentary throughout its anterolateral surface, and the angular ventrally and posterolaterally. The surangular portion of the articular complex is robust and mediolaterally thickened. It is bound ventrally by the deep adductor fossa. In lateral view, the mandibular foramen is encapsuled by two distinct ridges, one dorsal and one ventral. The ventral ridge further marks the dorsal margin of the articular facet with the angular. The articular is well developed, with a well-marked anteroposteriorly elongated ridge as articular area for the quadrate, as in other derived rhynchocephalians. This ridge is markedly anteroposteriorly convex dorsally and the articular facet is dorsoventrally deep. The retroarticular process is triangular in lateral and medial views. It is long and directed posteriorly with a slight dorsal bow. The retroarticular process tapers to a point posteriorly.

5.2.6 | Dentition

Among the preserved bones that can be clearly identified, teeth are only present on the dentaries. The pterygoids are edentulous.

There are 15 acrodont teeth on each dentary of SNSB-BSPG 2018 I 179, all exposed in lingual view. The teeth vary in size, with an overall size increase toward the

distal teeth. All teeth are additional teeth, there is no hatchling dentition or successional teeth. The mesial teeth are triangular, with slightly distally oriented tips and low anterior flanges. Teeth 3, 4, and 5 show a low posterior flange as well. Marked wear facets are absent in the tooth row. The four posteriormost teeth are the largest in the whole tooth row. They share a similar morphology with the anterior teeth, but with more defined and longer anterior flanges. These teeth are well spaced, with their anterior flanges ending far from the preceding tooth. The four posteriormost teeth are lodged in a sort of "pseudo-socket," composed of dentary bone that envelops the tooth bases. A large toothless region lies between the last tooth and the coronoid process. No striations can be seen on the lingual surface of the dentary teeth.

5.3 | Hyoid

A pair of long rod-like bones can be interpreted as ceratobranchials. These are slightly bowed and wider than the ribs (Figures 1 and 2). Their length-to-diameter proportions range from 0.07 to 0.08, and their length-to-mandible-length proportions range from 0.38 to 0.39.

5.4 | Axial skeleton

5.4.1 | General features

The preserved elements of the axial skeleton of SNSB-BSPG 2018 I 179 are completely disarticulated (Figures 1 and 4). A total vertebral count cannot be given, especially as the skeleton is incomplete posteriorly. There are at least 44 disarticulated neural arch pedicels, three disarticulated cervical ribs, and 63 disarticulated dorsal ribs, which would make the presacral vertebral count to a minimum of 39 vertebrae, assuming the presence of seven to eight cervical vertebrae (the number of cervicals known in other rhynchocephalians, e.g., seven in *Pleurosaurus*, Dupret, 2004; eight in *Sphenodon*, Hoffstetter & Gasc, 1969). Only presacral vertebrae are preserved, with no evidence of sacral or caudal ones. This is also supported by the presence of free dorsal ribs and gastralia associated with the posteriormost preserved region of the skeleton.

5.4.2 | Presacral vertebrae

The centra are amphicoelous and slightly longer than wide. They are constricted at their mid-length, resulting in an hourglass shape. A shallow longitudinal groove is present along the ventral surface of the centra. The synapophyses are well developed and expanded laterally. Left and right halves of the neural arch pedicels are unfused to each other and to the vertebral centrum (Figure 4a). The pre- and postzygapophyses are triangular in lateral view, with the former having a straight dorsal margin, parallel to the long axis of the vertebrae. The neural spine is tall and squared in lateral view. The anterior and dorsal margins of the spine are slightly convex, and the posterior one is concave.

5.4.3 | Ribs

At least three free cervical ribs are preserved. These ribs are short compared to the dorsal ribs, and more gracile. The free dorsal ribs are long, slender, and thin anteroposteriorly. A furrow is present throughout their length on the anterior surface. All ribs have a single, dorsoventrally extended facet for the articulation with the related synapophysis. Just distal to the articulation, the dorsal ribs show a dorsal concavity, before bowing ventrally.

5.4.4 | Gastralia

The gastralia are poorly preserved. They are long and thin bones composed by two rod-like arms that are deflected posterolaterally. These arms meet at the midline, forming a prominent anterior expansion. The posterior margin of the gastralia forms an obtuse angle between both arms.

5.5 | Appendicular skeleton

5.5.1 | General features

Most bones of the appendicular skeleton are not preserved. The preserved bones are disarticulated and displaced (Figures 1 and 4). SNSB-BSPG 2018 I 179 preserves the interclavicle, the left scapula, both coracoids, both humeri, the right radius, the right ulna, and an isolated bone interpreted as a metacarpal.

5.5.2 | Interclavicle

The interclavicle (Figure 4a,b) is preserved and exposed in ventral view. This bone is T-shaped, with its paired lateral processes being gently bowed and slightly posteriorly inclined. The anterior margin of the interclavicle bears a wide and shallow concavity in the middle. The median shaft is short and there is a low

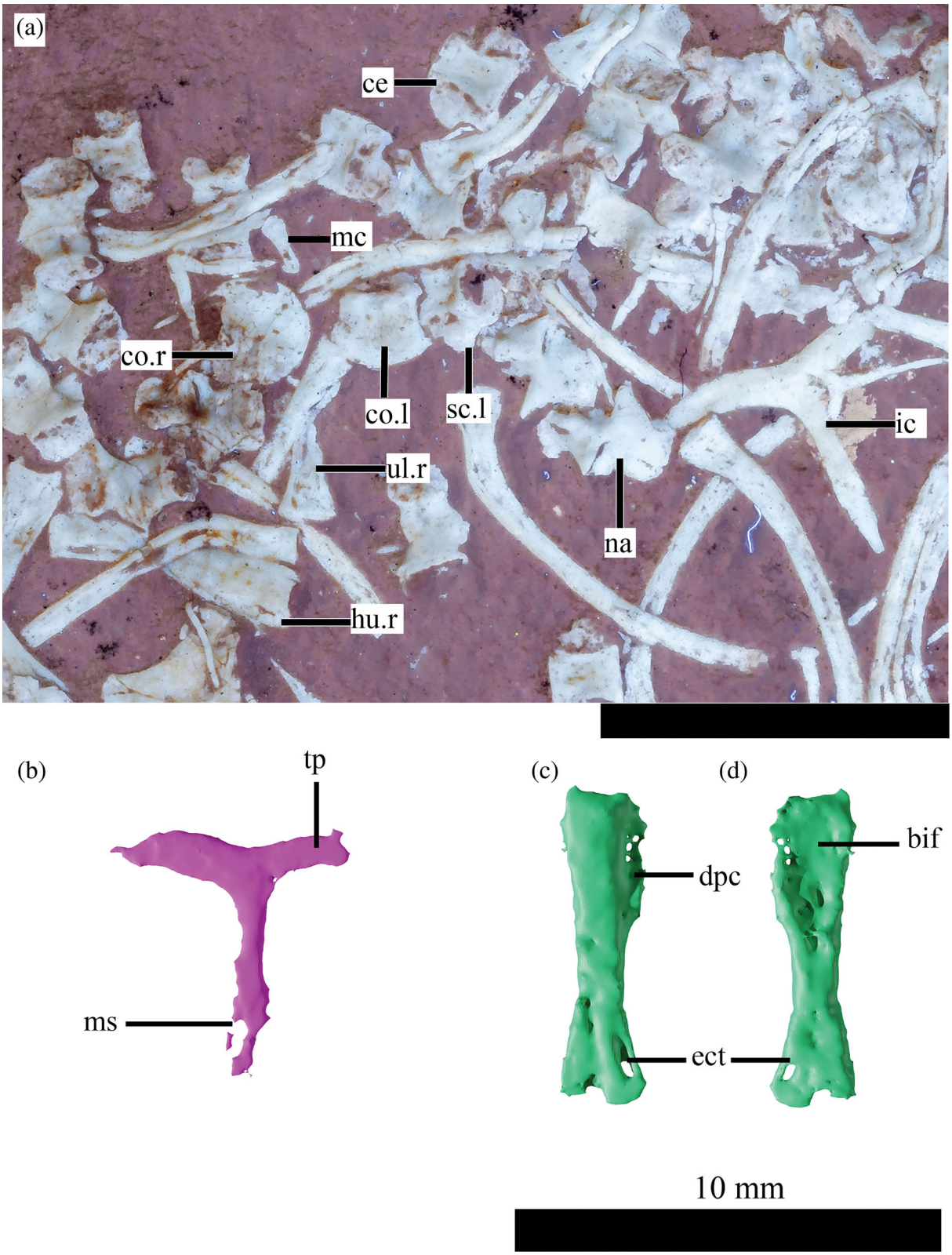

FIGURE 4 Selected postcranial bones of *Pleurosaurus* cf. *P. ginsburgi* SNSB-BSPG 2018 I 179. (a) Photograph under UV light of disarticulated postcranial bones; (b–d) 3D representation of (b), interclavicle in ventral view; (c) right humerus in posterior view; (d) right humerus in anterior view. All scale bars = 10 mm. bif, bicipital fossa; ce, centrum; co, coracoid; dpc, deltopectoral crest; ect, ectepicondylar foramen; hu, humerus; ic, interclavicle; mc, metacarpal; ms, median shaft; na, neural arch; sc, scapula; tp, transverse process; ul, ulna; l, left; r, right.

lateral expansion at its midlength. The length of the shaft is similar to that of one of the lateral processes, just being slightly longer.

5.5.3 | Scapula and coracoid

Both coracoids and the left scapula are preserved and exposed in lateral view (Figure 4a). The scapula is unfused to the coracoid. It is smaller than the coracoid and ovoid in lateral view, and wider than tall. The coracoid is as wide as tall, with a strongly convex anterior margin. Both the scapula and coracoid contribute evenly to the glenoid fossa, which is large, slightly laterally directed and covers approximately three fourths of the height of the contact between coracoid and scapula.

5.5.4 | Humerus

Both humeri are preserved but obscured by other bones. The best preserved humerus is the right one, which is preserved in posterior view (Figure 4c,d). The humerus is the largest forelimb bone in SNSB-BSPG 2018 I 179. The proximal and distal ends of the humerus are not twisted, with the bicipital fossa in the same plane as the distal condyles. Both proximal and distal epiphyses are poorly ossified, with the proximal end of the humerus being concave. The deltopectoral crest is shallow and only slightly anteriorly expanded. The shaft is constricted, which makes the humerus slightly hourglass-shaped. At the distal end, the ecte- and entepicondyles are separated by a distal concavity. The ectepicondylar foramen opens both anterior and posteriorly. The entepicondylar foramen cannot be observed in this specimen due to its preservation.

5.5.5 | Other forelimb bones

The proximal portion of the right ulna, as well as the right radius are poorly preserved. The proximal end of the ulna is expanded dorsoventrally. A shallow fossa lies between this expansion. The olecranon is possibly unossified and not preserved. Nothing can be said about the distal end of the ulna. The radius is elongated and expanded at the proximal and distal ends. Its shaft is slightly bowed. The radius has approximately two-thirds of the humerus length.

A single isolated metacarpal is preserved in dorsal view. It is slender, wider proximally and distally. The proximal end is convex and expands more lateromedially than the distal end. It is not possible to confidently assign the position of this bone within the hand, but its slender build suggests that it is one of metacarpals II–IV (e.g., Cocude-Michel, 1963; Lee et al., 2016).

5.6 | Skeletal reconstruction and SL assessment

The CT-scan of SNSB-BSPG 2018 I 179 allowed for the individual bones to be separated and reassembled digitally. The reassembled skull and mandible (Figure 5a–d) help in the visualization of the specimen and proper comparison to other *Pleurosaurus* specimens (Figure 5e–j). Most bones are taphonomically distorted, having been flattened and compressed. Therefore, the reconstruction does not represent the actual proportions or shape of the bones of the specimen in life.

Due to the missing anterior region of the skull, it is not possible to measure the full SL. However, with the generation of similar models for adult specimens of closely related taxa (*P. ginsburgi* and *P. goldfussi*), we see that their SL varies from 0.88 to 0.91 of the mandible length. Using this proportion to scale the skull of SNSB-BSPG 2018 I 179 based on its complete mandible, the specimen should have a SL that ranges from 38 to 39.5 mm. Our 3D reconstructions confirm a more dorsal position of the jaw joint compared to the plane corresponding to the long axis of the maxillary tooth row in *Pleurosaurus*, as already reported by Jones (2008). Nevertheless, these comparisons should be seen with caution as we still know little of the variation in the skull proportions of pleurosaurids (with the exception of fenestrae-to-skull proportions; see Fabre, 1981) and skull proportions among specimens of *Sphenodon*, particularly during ontogeny, are significantly variable (e.g., Jones et al., 2009).

6 | DISCUSSION

6.1 | Taxonomical assignment

Although incomplete, SNSB-BSPG 2018 I 179 shows significant differences from non-pleurosaurid rhynchocephalians, as well as some pleurosaurids. It differs from *Derasmosaurus*, *Homoeosaurus* (except for a single specimen, NHMUK PV R 2741; Cocude-Michel, 1963; Fabre, 1981; VB, personal observation), *Oenosaurus, Sapheosaurus*, *Sphenodon*, and *Sphenofontis* due to the narrow and shallow streamlined profile of the skull (Cocude-Michel, 1963; Evans, 2008; Fabre, 1981; Rauhut et al., 2012; Villa et al., 2021). It differs from *Homoeosaurus* (NHMUK PV R 2471), *Kallimodon*, *Leptosaurus*, *Palaeopleurosaurus*, and *Vadasaurus* in having a slender,

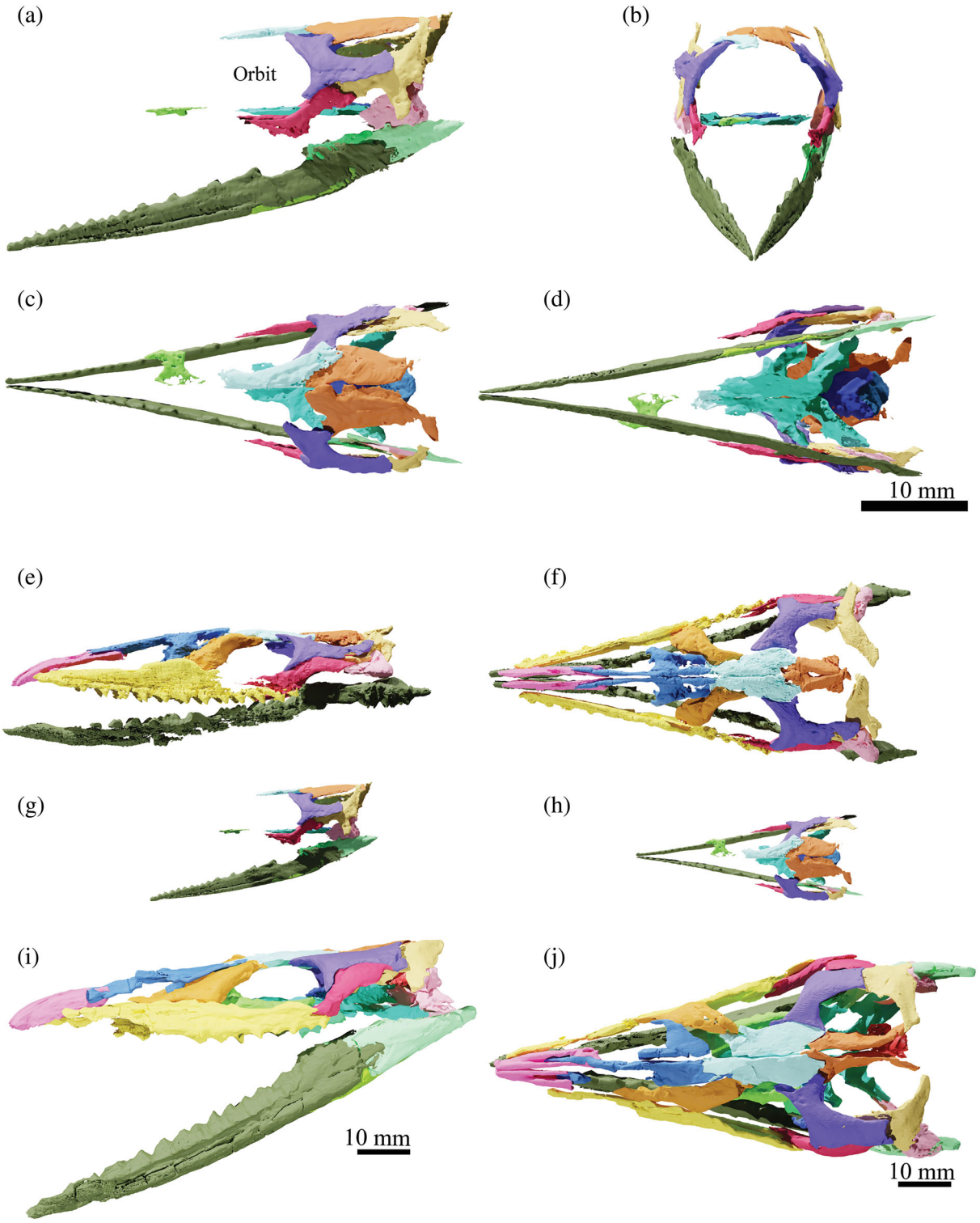

FIGURE 5 Skull comparison of 3D reconstructed *Pleurosaurus* specimens from the SNSB-BSPG. (a–d) Digital reconstruction of the skull of SNSB-BSPG 2018 I 179 in (a), left lateral view; (b) anterior view; (c) dorsal view; (d) ventral view. (e, f) *Pleurosaurus ginsburgi* SNSB-BSPG 1978 I 7, subadult, in left lateral and dorsal view; (g, h) *Pleurosaurus* cf. *P. ginsburgi* SNSB-BSPG 2018 I 179, juvenile, in left lateral and dorsal view; (i, j) *Pleurosaurus goldfussi* SNSB-BSPG 1925 I 18, adult, in left lateral and dorsal view.

elongated lower jaw with straighter dorsal and ventral margins (Bever & Norell, 2017; Carroll, 1985; Cocude-Michel, 1963; Fabre, 1981). It lacks a caudal (quadratojugal) process on the jugal which is present to a variable degree in *Diphydontosaurus* Whiteside, 1986, *Planocephalosaurus* Fraser, 1982, *Clevosaurus* Swinton, 1939, *Opisthiamimus*

DeMar et al., 2022, and *Sphenodon* (DeMar et al., 2022; Jones, 2008; O'Brien et al., 2018). It is further distinguished from all these taxa according to dentary tooth structure: the teeth are triangular in lingual view, with low anterior flanges. The elongated anteromedial process of the coronoid of SNSB-BSPG 2018 I 179 differs from the short one in *Sphenofontis* (Villa et al., 2021). Differently from *Tingitana*, the dentition of SNSB-BSPG 2018 I 179 lacks the robust posterior cones with anterolingually oriented flanges (Evans & Sigogneau-Russell, 1997). SNSB-BSPG 2018 I 179 also lacks the additional groove dorsal to the Meckelian fossa on the medial side of the dentary found in the Moroccan taxon (Evans & Sigogneau-Russell, 1997). The retroarticular process of SNSB-BSPG 2018 I 179 is elongated posteriorly, different from the short retroarticular process of *Navajosphenodon* Simões et al., 2022, *Oenosaurus, Sphenodon*, and *Sphenofontis* (Evans, 2008; Rauhut et al., 2012; Simões et al., 2022; Villa et al., 2021). The interclavicle of SNSB-BSPG 2018 I 179 has a short median process with lateral expansions at its mid-length, differing from the straight, tubular and long process of *Kallimodon*, *Sphenodon*, and *Sphenofontis* (Cocude-Michel, 1963; Russell & Bauer, 2008; Villa et al., 2021). The lateral processes of the interclavicle (transverse processes in Dupret, 2004) are bowed slightly posteriorly, as was described for *P. goldfussi* (Dupret, 2004; Villa et al., 2021), different from the straight lateral processes of *Kallimodon* (SNSB-BSPG 1922 I 15), *Sphenodon*, and *Sphenofontis* (Cocude-Michel, 1963; Russell & Bauer, 2008; Villa et al., 2021).

The new specimen described here presents a set of osteological features that allows its classification as *Pleurosaurus*. It can be assigned to Pleurosauridae (sensu Dupret, 2004) due to the presence of an elongated and triangular skull and the elongated axial skeleton (at least 39 presacral vertebrae). SNSB-BSPG 2018 I 179 differs from *Palaeopleurosaurus* in having a more gracile, elongated lower jaw with almost straight dorsal and ventral margins, taller and squared neural spines in lateral view, opposed to the short, rhomboidal neural spines of *Palaeopleurosaurus* (Carroll, 1985), and over 39 presacral vertebrae, opposed to 37 in *Palaeopleurosaurus* (Carroll, 1985; Dupret, 2004). The Specimen SNSB-BSPG 2018 I 179 differs from *Vadasaurus* in missing a free postfrontal (it being either fused to the postorbital, fused to the frontal, or absent in SNSB-BSPG 2018 I 179) and surangular–articular–prearticular (articular complex), as well as in the higher number of presacral vertebrae (Bever & Norell, 2017).

The specimen can be assigned to the genus *Pleurosaurus* due to the low anterior flanges on its dentition. Another diagnostic feature of *Pleurosaurus* is the absence of a separate postfrontal, which is also the case in the specimen SNSB-BSPG 2018 I 179. There are at least two features that have not been proposed as diagnostic characters for *Pleurosaurus* but seem to be present exclusively in specimens assigned to this genus and also in SNSB-BSPG 2018 I 179. The bifid anterior process of the jugal, present also in SNSB-BSPG 1925 I 18, SNSB-BSPG 1977 X 40, and SNSB-BSPG 1978 I 7, and at least some of the dentary teeth inserted into shallow "pseudosockets," present also in SNSB-BSPG 1977 X 40 and SNSB-BSPG 1978 I 7.

The humeral length (HL) of SNSB-BSPG 2018 I 179 is 0.18–0.19 of the SL, which is a diagnostic characteristic of *P. ginsburgi* (sensu Dupret, 2004, but see Section 4.2). However, proper assignment to any of the known *Pleurosaurus* species is hindered by the absence of some skull bones such as the upper jaw elements and nasals, and disarticulation of the skull (making it impossible to measure the relationships between the skull openings and total SL, significant features to discriminate between *Pleurosaurus* species; Fabre, 1981; Dupret, 2004). Therefore, SNSB-BSPG 2018 I 179 is only tentatively attributed here to *Pleurosaurus* cf. *P. ginsburgi*, as it best fits the proposed diagnosis of *P. ginsburgi* (Dupret, 2004; Fabre, 1974, 1981).

6.2 | *Pleurosaurus* taxonomic issues

The taxonomy of *Pleurosaurus* has been revised by Dupret (2004) and an emended diagnosis for both *Pleurosaurus* species was given in his study. According to this author, the main differences between *P. ginsburgi* and *P. goldfussi* are found in the presacral vertebral count and in the proportions between skull openings and bones. However, the taxonomic significance of at least some of these diagnostic characters may be questioned. The vertebral count is known to be a sexually dimorphic feature in other lepidosaurs, such as, for example, in some squamates (skinks: Choquenot & Greer, 1989; Greer, 1990; lacertids: Kaliontzopoulou et al., 2008; geckos: Kratochvíl et al., 2018), and some specimens of the extant tuatara can have 24 presacral vertebrae, contrary to the usual 25 (Howes & Swinnerton, 1901; Hoffstetter & Gasc, 1969; VB, personal observations). The skull proportion variation could be explained by ontogenetic or intraspecific variation, as is the case for *Sphenodon* (Jones, 2008). In *Sphenodon*, the orbit-to-SL proportions change during ontogeny, with the postorbital area increasing in size when compared to the preorbital area (Jones, 2008). Regarding the humerus-to-SL proportions, another proposed diagnostic characteristic for *Pleurosaurus* species, in *Sphenodon* we see a negative allometry trend for the humerus length compared to the SL (slope = 0.88331, $r^2 = 0.94977$, $p < 0.01$; VB, preliminary analysis and observation). If this is also the case for *Pleurosaurus*, we would expect that the proportions between humerus and SL vary

throughout ontogeny, and thus they cannot be considered a reliable diagnostic character. Specimens such as SNSB-BSPG 1977 X 40 and SNSB-BSPG 1978 I 7 have 59 presacral vertebrae, which is closer to *P. ginsburgi* (even though differing slightly from the proposed diagnostic 57 presacral vertebrae of Dupret, 2004) than to *P. goldfussi* (50 presacral vertebrae). However, SNSB-BSPG 1977 X 40 shows a humeral to SL proportions value over 0.2 (HL/SL = 0.28), which is diagnostic for *P. goldfussi* (still according to Dupret, 2004). Two specimens assigned to *P. goldfussi* indeed show HL/SL higher than 0.2, with values of 0.28 and 0.38 (specimen housed in the Muséum d'Histoire Naturelle de Lyon, reported as 15,640 by Dupret, 2004, and SNSB-BSPG 1925 I 18, respectively). The proportions calculated for the French specimen are the same as that of SNSB-BSPG 1977 X 40, implying a more complex distribution of the supposedly diagnostic features.

In his study, Dupret (2004) used only a few specimens of *Pleurosaurus*, and no variability analysis was made. We suggest that a systematic and comprehensive revision of *Pleurosaurus* specimens should be carried out to understand which features might be related to intra- or interspecific variation and to properly define the two (or more) species in this genus and the related diagnostic features. Indeed, we can observe morphological differences between *Pleurosaurus* specimens that are potentially due to interspecific variation, for example the elongated premaxilla and slender ascending process of the jugal in SNSB-BSPG 1978 I 7 (Figure 5e,f) against the proportionally short and robust premaxilla and deep ascending process of the jugal of SNSB-BSPG 1925 I 18 (Figure 5i,j). However, differences in size between these two specimens (SNSB-BSPG 1925 I 18 is slightly larger than SNSB-BSPG 1978 I 7) should be also taken into account when evaluating potential involvement of ontogenetic variation in the development of such features. Also, considering that the ascending process of the jugal is even more slender in the small SNSB-BSPG 2018 I 179, interpreted as an early juvenile here (see below), the three specimens could be aligned in a matching pattern of increasing robustness of this bone and overall size of the animal.

Another aspect to consider is the different stratigraphic distribution of the specimens included in the genus *Pleurosaurus*. In the case of the aforementioned specimens SNSB-BSPG 1978 I 7 and SNSB-BSPG 1925 I 18, the former comes from the Mörnsheim Formation at Daiting, whereas the latter is from the Altmühltal Formation of Sappenfeld, near Eichstätt, and thus probably some hundreds of thousand years older. In general, the genus *Pleurosaurus* has been recorded from units in southern Germany and France spanning from the *Pseudomutabilis* ammonite zone of the Late Kimmeridgian (locality Wattendorf; Mäuser, 2015) to the higher Early Tithonian of the Mörnsheim Formation, like the specimen described here (*Moernsheimensis* subzone of the *Hybonotum* ammonite zone; Schweigert, 2015), and even the younger *Mucranotum* biozone of the Calcaires blancs de Provence Formation (locality Canjuers; Peyer et al., 2014). Thus, at least some of the differences seen might also be due to anagenetic changes in a single evolving lineage. In any case, an improved diagnosis for the genus *Pleurosaurus* and its species falls outside the scope of the current work, and we highly anticipate future works on the topic.

6.3 | Ontogenetic assignment

There are some caveats when assessing the ontogeny of *Pleurosaurus* specimens that should be taken into consideration to assign SNSB-BSPG 2018 I 179 to a specific ontogenetic stage. Adult *Pleurosaurus* usually retain "juvenile" morphological features, such as in the late fusion of neural arches with the related vertebral centra (Figure 6), unfused scapulocoracoid, pelvic girdle, and astragalocalcaneum, and poorly ossified (cartilaginous) epiphyses in limb bones (Cocude-Michel, 1963; Fabre, 1974; Carroll, 1985; Reynoso, 2000; Dupret, 2004; Bever & Norell, 2017; Simões et al., 2020 supplementary data 2), although some of these features (i.e., unfused girdles and astragalocalcaneum, and poorly ossified epiphyses) are common feature of aquatic tetrapods (Bever & Norell, 2017; Lee et al., 2016; Reynoso, 2000). Nevertheless, SNSB-BSPG 2018 I 179 shows a set of features not found in any *Pleurosaurus* specimen assigned to later ontogenetic stages (e.g., subadults and adults), including: (1) almost unworn dentition; (2) a large gap between the last dentary tooth and the coronoid process, given that the last tooth lies immediately anterior to the coronoid process in subadult and adult *Pleurosaurus* specimens such as SNSB-BSPG 1925 I 18 (Figure 5i,j), SNSB-BSPG 1977 X 40 (Figure 6g–i), and SNSB-BSPG 1978 I 7 (6D-F); (3) widely-spaced and well-separated posteriormost teeth, different from the condition in adult *Pleurosaurus* (i.e., almost overlapping teeth, as seen in MNHN 1983-4 CNJ 67, SNSB-BSPG 1925 I 18, SNSB-BSPG 1977 X 40, and SNSB-BSPG 1978 I 7, Fabre et al., 1982; Dupret, 2004; VB, personal observations); and (4) presacral neural arches still represented by unfused pedicels. It is worth noting that the placement of dentary teeth relative to the coronoid process of the dentary seems to be an ontogenetic feature exclusive to *Pleurosaurus*. Although a similar placement of the dentition has been suggested as an ontogenetic factor in *Sphenodon* (e.g., Harrison, 1901; Howes & Swinnerton, 1901; Rieppel, 1992; Simões et al., 2022), our preliminary evaluation of the ontogenetic series of *Sphenodon* shows that the

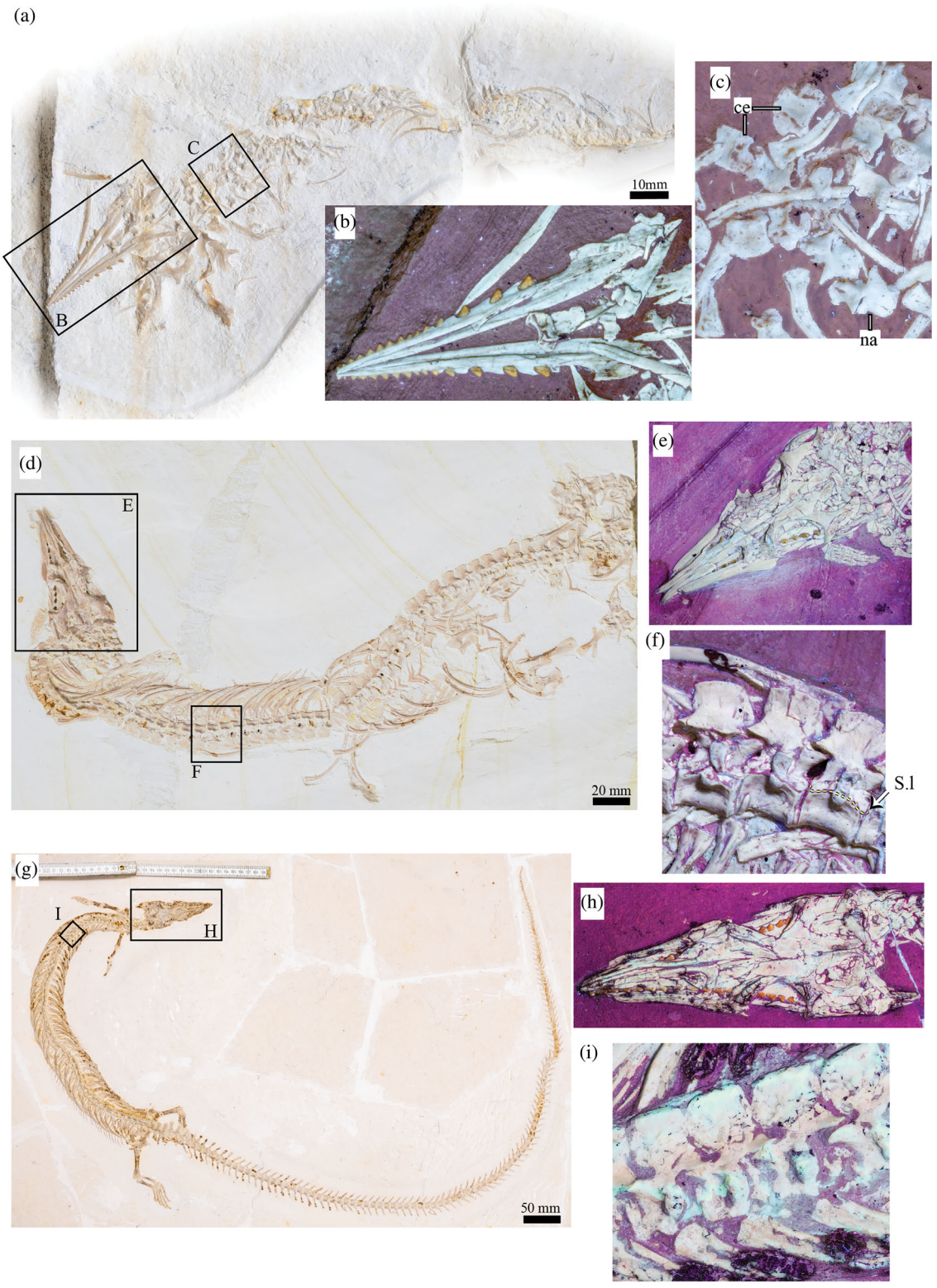

FIGURE 6 Comparison of *Pleurosaurus* specimens from the SNSB-BSPG. *Pleurosaurus* cf. *P. ginsburgi* SNSB BSPG 2018 I 179, juvenile (a–c); *Pleurosaurus ginsburgi* SNSB BSPG 1978 I 7, possibly subadult due to the visible suture between neural arches and centra in the presacral vertebrae (d–f); *Pleurosaurus ginsburgi* SNSB BSPG 1977 X 40, adult with fully ossified vertebrae (g–i). (a), (d), and (g), photographs in standard light; (b, c); (e, f); and (h, i) photographs under UV-light of details, that is, dentition, and presacral vertebrae. Ce, presacral vertebra centrum; na, presacral vertebra neural arch, S.l, suture line.

gap between the distalmost dentary tooth and the coronoid process increases throughout ontogeny, as is also the case for *Clevosaurus brasiliensis* Bonaparte & Sues, 2006 (see Chambi-Trowell et al., 2021).

Given that skulls of adult *Pleurosaurus* specimens, regardless of species identity, typically range between 80 and 110 mm in length (e.g., Broili, 1926; Cocude-Michel, 1963, 1967; Fabre, 1981; Von Huene, 1952), the animal described here was, at best, half the size of an adult representative of that genus. Furthermore, other small and presumably juvenile specimens of *Pleurosaurus* described or mentioned in the literature (Dames, 1896; Von Huene, 1952) have skulls that are at least 25% larger than the specimen described here, making this the smallest known specimen that can be securely referred to this genus so far. Therefore, we can confidently assign SNSB-BSPG 2018 I 179 to an early (post-hatchling) juvenile stage, making it the probably youngest unambiguous juvenile specimen of *Pleurosaurus* described so far.

The interpretation of SNSB-BSPG 2018 I 179 as an early juvenile has some implications for the ontogeny of *Pleurosaurus*. This specimen shows that both the lack of a separate postfrontal (possibly due to fusion of this bone with either the postorbital or frontal) and the fusion of posterior mandibular bones (i.e., surangular, articular, and prearticular) into an articular complex both occur early in the development of *Pleurosaurus*, possibly even at a pre-hatchling stage. This has taxonomical value, as closely related taxa known from late ontogenetic stage specimens, such as *Vadasaurus* and *Palaeopleurosaurus*, show separate postorbital and postfrontal, as well as unfused mandibular bones (Bever & Norell, 2017; Carroll, 1985).

6.4 | Functional interpretations

The presence of robust ceratobranchials in SNSB-BSPG 2018 I 179, as well as other morphological features such as an elongated presacral skeleton and reduced forelimbs, argue for an aquatic lifestyle (Bever & Norell, 2017; Delsett et al., 2023; Lee et al., 2016; Reynoso, 2000). The relatively large hyoid bones suggest that food was acquired within the water column. These bones would be potentially used as part of the hyolingual apparatus to generate negative pressure within the mouth and capture food items including perhaps even elusive prey such as fish (as reported for turtles by Lemell et al., 2019). This would indicate that *Pleurosaurus* were marine dwellers from an early ontogenetic stage. It has been proposed previously that *Pleurosaurus* could have been viviparous animals (Blackburn & Sidor, 2014), and the presence of early juvenile specimens in aquatic environments provides support for this idea. However, at this moment, no known specimen of gravid *Pleurosaurus* has been reported to corroborate this claim.

6.5 | *Acrosaurus* as a possible *Pleurosaurus* hatchling

Acrosaurus frischmanni specimens are abundant in the Solnhofen Archipelago limestones (e.g., Cocude-Michel, 1963; Fabre, 1981), albeit not to the same extent as *Pleurosaurus*. They range in age from Late Kimmeridgian to Early Tithonian from the Torleite Formation to the Mörnsheim Formation, thus sharing the same stratigraphic distribution as the Solnhofen Archipelago *Pleurosaurus* (Cocude-Michel, 1963; Rauhut & López-Arbarello, 2016; Tischlinger & Rauhut, 2015). *Acrosaurus frischmanni* specimens, however, are usually poorly preserved and hard to describe. All specimens of *A. frischmanni* observed (i.e., the holotype SNSB-BSPG AS I 564; SNSB-BSPG 1953 I 431; SNSB-BSPG 1953 88; TM F06931; and an undescribed private specimen from Painten, Germany, OWMR, personal observation) seem to be poorly ossified and show clear indications of being skeletally immature individuals (i.e., unworn dentition, poorly ossified skulls, unfused neural arches in the axial skeleton, and poorly ossified limb bones).

The holotype of *A. frischmanni* (SNSB-BSPG AS I 564; Figure 7) shows many of the diagnostic features of *Pleurosaurus* (sensu Dupret, 2004), and especially of *P. goldfussi*, such as the low anterior flange in the mandibular dentition (Figure 7b), 49 presacral vertebrae (although this number could be underestimated due to the poor preservation of the skeleton), and a humerus to SL proportion greater than 0.2 (being 0.23 in this specimen). This specimen is morphologically similar to SNSB-BSPG 2018 I 179, which we refer here to *Pleurosaurus* cf. *P. ginsburgi*. The holotype of *A. frischmanni* differs from SNSB-BSPG 2018 I 179 mainly in size, but also in having taller and conical mesialmost teeth, opposed to triangular mesialmost teeth in SNSB-BSPG 2018 I 179, possibly separate postorbital and postfrontal bones (Figure 7b), fused neural arch pedicels (Figure 7c), and more developed, convex humeri epiphyses. Cocude-Michel (1963) considered *A. frischmanni* as a valid species, different from both *Pleurosaurus* species, due to a globular posterior region of the skull, dentition increasing in size posteriorly in the jaws, lack of ungual ventral "bumps", differences in their scale patterns, and a lower presacral vertebral count. The presacral vertebral count of the holotype of *A. frischmanni* is 49, similar to that of *P. goldfussi* (50 presacral vertebrae). The globular posterior region is a common feature in juveniles of other lepidosaurs, including the extant tuatara. The skull shape changes throughout ontogeny, with a

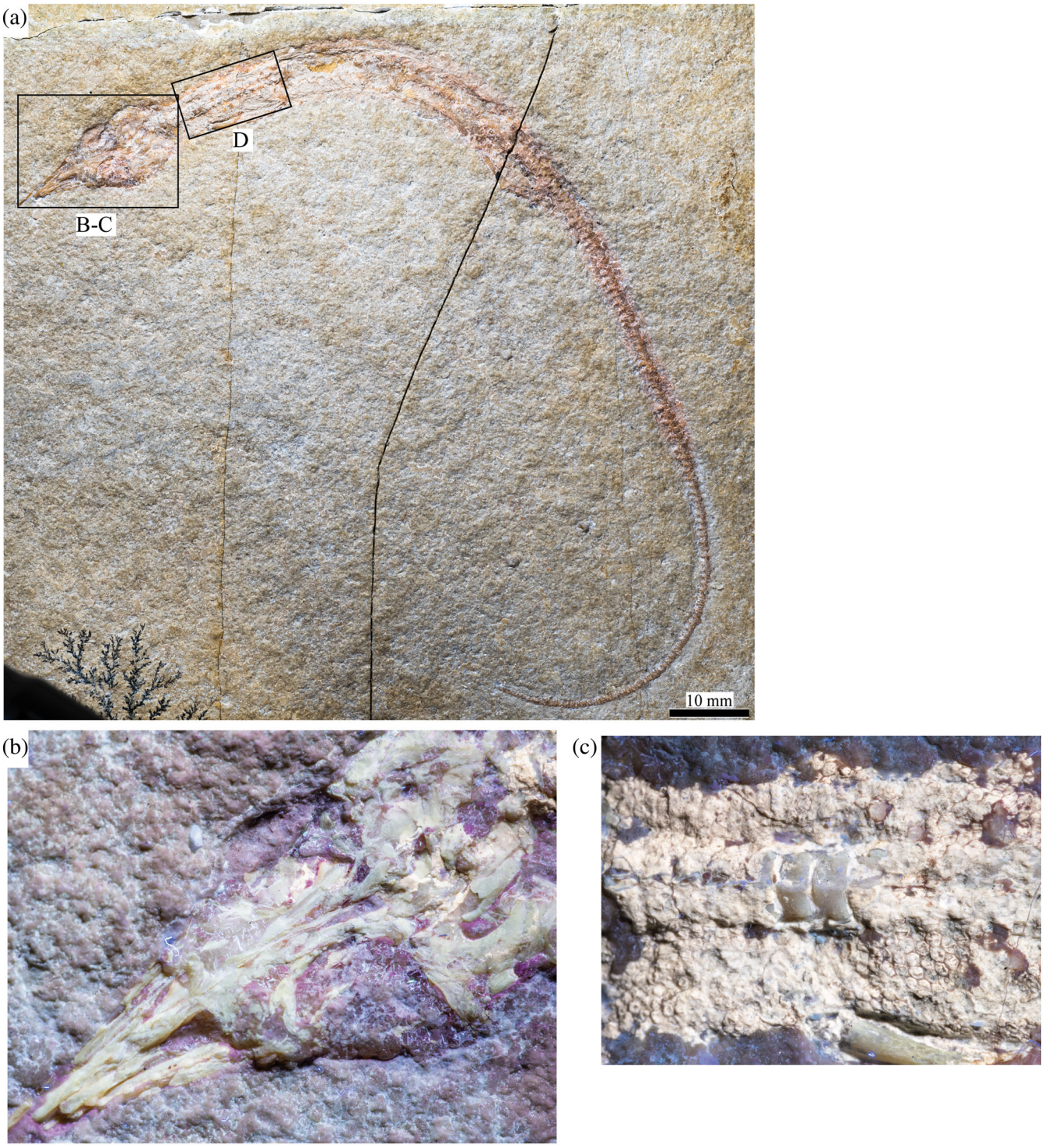

FIGURE 7 Notable features of the holotype of *Acrosaurus frischmanni* (SNSB-BSPG AS I 564). (a) Photograph of the holotype under standard light, (b) details of the skull of the holotype under UV light, and (c) details of the presacral vertebrae of the holotype under UV light.

relative elongation of the postorbital region of the skull compared to the anterior region (Jones, 2008). In his morphometric analysis of rhynchocephalian skull shapes, Jones (2008) used a reconstructed *Acrosaurus* skull from Rothery (2005) and recovered it as occupying a region of the morphospace close to that of *Pleurosaurus*, in a distance to each other similar to that between hatchling and adult *Sphenodon* specimens. The size of the teeth in *Pleurosaurus* also increases posteriorly in the jaws, as is the case in most rhynchocephalians that have posteriorly added additional teeth (see Robinson, 1976; Simões et al., 2022). Therefore, this is not a good diagnostic feature

for *A. frischmanni*. There are, however, some arguments related to ontogeny that favor the validity of *A. frischmanni*. The holotype of *A. frischmanni*, although possibly representing a young individual, shows a larger degree of ossification than SNSB-BSPG 2018 I 179, for example, the fused neural arch pedicels and the humeral epiphyses, especially the proximal one. In SNSB-BSPG 2018 I 179, the proximal epiphysis of the humerus is poorly developed and concave, whereas the proximal epiphysis of SNSB-BSPG AS I 564 is convex and well-defined. The neural spines of *A. frischmanni* are also anteroposteriorly shorter than in *Pleurosaurus*. The lack of a proper diagnosis for *Pleurosaurus* (as mentioned in Section 4.2) hampers any more definitive statement on the taxonomic status of this small rhynchocephalian species.

7 | CONCLUSIONS

Up to this point, few juvenile specimens of *Pleurosaurus* have been described. The new specimen of *Pleurosaurus* cf. *P. ginsburgi* (SNSB-BSPG 2018 I 179) from the Late Jurassic (Early Tithonian) of the Solnhofen Archipelago, Germany, that we report here, however, can be assigned to an early juvenile (post-hatchling) stage. This specimen is mostly disarticulated but preserves much of its skull and axial skeleton. Its partial completeness provides more data for understanding *Pleurosaurus* anatomy. The specimen shows the diagnostic features of *Pleurosaurus*, that is, elongated skull, triangular lower jaws in dorsal view, presence of a low anterior flange on the teeth, and high number of dorsal vertebrae (at least 39 presacral vertebrae in this specimen). It shows one further diagnostic feature of *P. ginsburgi*, a humerus-to-SL proportion lower than 0.20. However, there are many issues with the current taxonomy of the genus *Pleurosaurus* and its two currently described species. Therefore, the lack of proper diagnoses for *Pleurosaurus* species, which heavily rely so far on the relationships between skull openings and appendicular skeleton proportions, led us to consider our species assignment of this juvenile specimen only as tentative for the time being. There are, however, clear differences in the skeleton (especially in the cranium) of specimens assigned to either species of *Pleurosaurus* that could justify their taxonomical identity, such as the morphology of the premaxilla and jugals. Nevertheless, a new diagnosis of *Pleurosaurus* and the species it includes falls outside the scope of the current work.

The new specimen shows features indicative of a young ontogenetic stage, such as the retention of an intact (i.e., unworn) dentition and completely unfused neural arch pedicles in the presacral vertebrae. As such, this specimen probably represents the youngest post-hatchling juvenile pleurosaurid that can be unambiguously assigned to the genus *Pleurosaurus*. The importance of this ontogenetic assignment lies in the presence of features that can be recognized as possible new diagnostic characters for the genus *Pleurosaurus*, such as the loss or fusion early in ontogeny of the postfrontal and the fusion of the mandibular articular complex. The new specimen already shows many morphological features related to a marine lifestyle (i.e., robust ceratobranchials, streamlined skull, elongated presacral series, and reduced limbs), indicating that *Pleurosaurus* was already an aquatic animal early in its ontogeny.

Moreover, it has further implications for another rhynchocephalian genus from the Solnhofen Archipelago, *Acrosaurus*. This genus displays a set of morphological features that are diagnostic for *Pleurosaurus*, such as the low anterior flange on the teeth, the high presacral vertebral count (49 presacral vertebrae), and the relative size of the humerus compared to the SL. Most of the proposed diagnostic features for *A. frischmanni*, the only species within *Acrosaurus*, are not exclusive to this taxon or are possibly related to the ontogenetic stage of the specimens assigned to it. *Acrosaurus* can thus be interpreted as a junior subjective synonym of *Pleurosaurus*, even though specimens referred to this genus display juvenile features to an even higher degree than the *Pleurosaurus* specimen described in this study.

AUTHOR CONTRIBUTIONS

Beccari V: Conceptualization; investigation; funding acquisition; writing – original draft; methodology; visualization; software; formal analysis; data curation; resources. **Andrea Villa:** Investigation; writing – review and editing; validation; formal analysis; funding acquisition. **Marc E. H. Jones:** Investigation; validation; writing – review and editing; formal analysis. **Gabriel S. Ferreira:** Investigation; methodology; software; data curation; visualization; writing – review and editing; formal analysis. **Frank Glaw:** Investigation; writing – review and editing; validation; formal analysis; supervision. **Oliver W. M. Rauhut:** Investigation; writing – review and editing; validation; methodology; formal analysis; funding acquisition; project administration; supervision; data curation; resources.

ACKNOWLEDGMENTS

VB would like to thank the following colleagues for access to specimens: Anne Schulp and Tim de Zeeuw (TM); Rainer Brocke and Gunnar Riedel (SMF); Karin Peyer and Nour-Eddine Jalil (NHMN); Michael O. Day and Susannah Maidment (NHMUK); Rebecca Hunt-Foster

(DM); Maureen Walsh and Nathan Smith (NHMLA); and Daniel Brinkman and Vanessa Rhue (YB). The authors would like to thank the reviewers Sophie A. V. Chambi-Trowell and Flávio Pretto, as well as the editor Leonardo Kerber, for their comments which improved the current manuscript. VB is financed by DFG (10.13039/501100001659 – Deutsche Forschungsgemeinschaft) grant RA 1012/28-1. AV was supported by a Humboldt Research Fellowship from the Alexander von Humboldt Foundation during part of the development of this work; he is now funded by Secretaria d'Universitats i Recerca of the Departament de Recerca i Universitats, Generalitat de Catalunya, through a Beatriu de Pinós postdoctoral grant (2021 BP 00038). AV further acknowledges support by the CERCA Programme/Generalitat de Catalunya and the Agència de Gestió d'Ajuts Universitaris i de Recerca of the Generalitat de Catalunya (2021 SGR 00620). The authors acknowledge the support of the 3D Imaging Lab of the University of Tübingen and the Senckenberg Centre for Human Evolution and Palaeoenvironment for instrument use, and scientific and technical assistance. Open Access funding enabled and organized by Projekt DEAL.

ORCID

Victor Beccari https://orcid.org/0000-0003-2657-5702
Oliver W. M. Rauhut https://orcid.org/0000-0003-3958-603X

REFERENCES

Apesteguía, S. (2016). Rhynchocephalians: The least known South American lepidosaurs. In F. Agnolin, G. Lio, F. Brisson Egli, N. R. Chimento, F. E. Novas (Eds.) *Historia Evolutiva y Paleobiogeográfica de los vertebrados de América del Sur*, (vol. 6, pp. 7–19).

Barbera, C., & Macuglia, L. (1988). Revisione dei tetrapodi del Cretacico inferiore di Pietraroia (Matese orientale, Benevento) appartenenti alla collezione Costa del Museo di Paleontologia dell'Università di Napoli. *Memorie della Societa Geologica Italiana*, *41*, 567–574.

Bever, G. S., & Norell, M. A. (2017). A new rhynchocephalian (Reptilia: Lepidosauria) from the Late Jurassic of Solnhofen (Germany) and the origin of the marine Pleurosauridae. *Royal Society Open Science*, *4*(11), 170570. https://doi.org/10.1098/rsos.170570

Blackburn, D. G., & Sidor, C. A. (2014). Evolution of viviparous reproduction in Paleozoic and Mesozoic reptiles. *The International Journal of Developmental Biology*, *58*(10–12), 935–948. https://doi.org/10.1387/ijdb.150087db

Bonaparte, J. F., & Sues, H.-D. (2006). A new species of *Clevosaurus* (Lepidosauria: Rhynchocephalia) from the Upper Triassic of Rio Grande do Sul, Brazil. *Palaeontology*, *49*(4), 917–923. https://doi.org/10.1111/j.1475-4983.2006.00568.x

Broili, F. (1926). Ein neuer Fund von *Pleurosaurus* aus dem Malm Frankens. *Abhandlungen der Bayerischen Akademie der Wissenschaften*, *30*(8), 1–48.

Carroll, R. L. (1985). A pleurosaur from the Lower Jurassic and the taxonomic position of the Sphenodontida. *Palaeontographica. Abteilung A, Paläozoologie, Stratigraphie*, *189*(1–3), 1–28.

Carroll, R. L., & Wild, R. (1994). Marine members of the Sphenodontia. In N. C. Fraser & H.-D. Sues (Eds.), *In the shadow of the dinosaurs: Early Mesozoic tetrapods* (pp. 70–83). Cambridge University Press.

Chambi-Trowell, S. A. V., Martinelli, A. G., Whiteside, D. I., de Vivar, P. R. R., Soares, M. B., Schultz, C. L., Gill, P. G., Benton, M. J., & Rayfield, E. J. (2021). The diversity of Triassic South American sphenodontians: A new basal form, clevosaurs, and a revision of rhynchocephalian phylogeny. *Journal of Systematic Palaeontology*, *19*(11), 787–820. https://doi.org/10.1080/14772019.2021.1976292

Choquenot, D., & Greer, A. E. (1989). Intrapopulational and interspecific variation in digital limb bones and presacral vertebrae of the genus *Hemiergis* (Lacertilia, Scincidae). *Journal of Herpetology*, *23*, 274–281.

Cocude-Michel, M. (1963). Les rhynchocéphales et les sauriens des calcaires lithographiques (Jurassique supérieur) d'Europe occidentale. *Publications du musée des Confluences*, *7*(1), 3–224. https://doi.org/10.3406/mhnly.1963.992

Cocude-Michel, M. (1967). Revision des rhynchocephales de la collection du Musee Teyler de Haarlem (Pays-Bas), II. *Proceedings of the Koninklijke Nederlandse Akademie van Wetenschappen B*, *70*, 547–555.

Dames, W. (1896). Beitrag zur Kenntnis der Gattung *Pleurosaurus* H. v. Meyer. *Sitzungsberichte der Königlich preußischen Akademie der Wissenschaften zu Berlin*, *42*, 1109.

Delsett, L. L., Pyenson, N., Miedema, F., & Hammer, Ø. (2023). Is the hyoid a constraint on innovation? A study in convergence driving feeding in fish-shaped marine tetrapods. *Paleobiology*, *49*(4), 684–699. https://doi.org/10.1017/pab.2023.12

DeMar, D. G., Jones, M. E. H., & Carrano, M. T. (2022). A nearly complete skeleton of a new eusphenodontian from the Upper Jurassic Morrison Formation, Wyoming, USA, provides insight into the evolution and diversity of Rhynchocephalia (Reptilia: Lepidosauria). *Journal of Systematic Palaeontology*, *20*(1), 2093139. https://doi.org/10.1080/14772019.2022.2093139

Dupret, V. (2004). The pleurosaurs: Anatomy and phylogeny. *Revue de Paléobiologie, Genève*, *9*, 61–80.

Evans, S. E. (2008). The skull of lizards and tuatara. *Biology of Reptilia*, *20*, 1–347.

Evans, S. E., Prasad, G. V. R., & Manhas, B. K. (2001). Rhynchocephalians (Diapsida: Lepidosauria) from the Jurassic Kota Formation of India. *Zoological Journal of the Linnean Society*, *133*(3), 309–334. https://doi.org/10.1111/j.1096-3642.2001.tb00629.x

Evans, S. E., & Sigogneau-Russell, D. (1997). New sphenodontians (Diapsida: Lepidosauria: Rhynchocephalia) from the Early Cretaceous of North Africa. *Journal of Vertebrate Paleontology*, *17*(1), 45–51. https://doi.org/10.1080/02724634.1997.10010952

Fabre, J. (1974). Un squelette de *Pleurosaurus ginsburgi* nov. sp. (Rhynchocephalia) du Portlandien du Petit Plan de Canjuers (Var). *Comptes Rendus Hebdomadaires des Seances De L Academie des Sciences Series D*, *278*(19), 2417–2420.

Fabre, J. (1981). *Les rhynchocéphales et les ptérosauriens à crête pariétale du Kiméridgien supérieur-Berriasien d'Europe occidentale: Le gisement de Canjuers (Var-France) et ses abords* (p. 188). Éditions de la Fondation Singer-Polignac.

Fabre, J., Broin, F. d., Ginsburg, L., & Wenz, S. (1982). Les vertébrés du Berriasiende Canjuers (Var, France) et leur environnement. *Geobios*, *15*(6), 891–923. https://doi.org/10.1016/S0016-6995(82)80037-5

Fitzinger, L. J. (1840). Ueber *Palaeosaurus sternbergii*, eine neue Gattung vorweltlicher Reptilien. *Annalen des Wiener Museums der Naturgeschichte*, *2*, 171–187.

Fraser, N. C. (1982). A new rhynchocephalian from the British Upper Trias. *Palaeontology*, *25*(4), 709–725.

Goldfuss, G. A. (1831). *Beiträge zur Kenntnis verschiedener Reptilien der Vorwelt* (Vol. 15, pp. 61–128). Nova Acta Academiae Caesareae Leopoldino-Carolinae Germanicae Naturae Curiosorum.

Gray, J. E. (1831). Note on a peculiar structure in the head of an *Agama*. *Zoological Miscellany*, *1*, 13–14.

Gray, J. E. (1842). Description of two hitherto unrecorded species of reptiles from New Zealand; presented to the British museum by Dr. Dieffenbach. In *Zoological miscellany* (pp. 1–72). Treuttel, Würtz & Co.

Greer, A. E. (1990). Limb reduction in the scincid lizard genus *Lerista*. 2. Variation in the bone complements of the front and rear limbs and the number of postsacral vertebrae. *Journal of Herpetology*, *24*(2), 142–150. https://doi.org/10.2307/1564221

Günther, A. (1867). Contribution to the anatomy of *Hatteria* (*Rhynchocephalus*, Owen). *Philosophical Transactions of the Royal Society of London*, *157*, 595–629.

Haeckel, E. (1866). *Generelle Morphologie der Organismen. Allgemeine Grundzüge der organischen Formen-Wissenschaft, mechanisch begründet durch die von C. Darwin reformirte Descendenz-Theorie, etc* (Vol. 1). Verlag von Georg Reimer.

Harrison, H. S. (1901). The development and succession of teeth in *Hatteria Punctata*. *Journal of Cell Science*, *2*(174), 161–213.

Hay, J. M., Sarre, S. D., Lambert, D. M., Allendorf, F. W., & Daugherty, C. H. (2010). Genetic diversity and taxonomy: A reassessment of species designation in tuatara (*Sphenodon*: Reptilia). *Conservation Genetics*, *11*(3), 1063–1081.

Herrera-Flores, J. A., Stubbs, T. L., & Benton, M. J. (2017). Macroevolutionary patterns in Rhynchocephalia: Is the tuatara (*Sphenodon punctatus*) a living fossil? *Palaeontology*, *60*(3), 319–328. https://doi.org/10.1111/pala.12284

Heyng, A., Rothgaenger, M., & Röper, M. (2015). Die Grabung Brunn. In G. Arratia, H.-P. Schultze, H. Tischlinger, & G. Viohl (Eds.), *Solnhofen: Ein Fenster in die Jurazeit* (pp. 114–118). Verlag Dr. Friedrich Pfeil.

Hoffstetter, R. (1955). Rhynchocephalia. In Pivetaut J, ed. *Traité de Paléontologie, T5 (Amphibiens, Reptiles, Oiseaux)*. (Vol. 5, pp. 556–576). Masson.

Hoffstetter, R., & Gasc, J.-P. (1969). Vertebrae and ribs of modern reptiles. *Biology of the Reptilia*, *1*(5), 201–310.

Howes, G. B., & Swinnerton, H. H. (1901). On the development of the skeleton of the tuatara, *Sphenodon punctatus*; with remarks on the egg, on the hatching, and on the hatched young. *The Transactions of the Zoological Society of London*, *16*(1), 1–84.

Hsiou, A. S., Nydam, R. L., Simões, T. R., Pretto, F. A., Onary, S., Martinelli, A. G., Liparini, A., Romo de Vivar Martínez, P. R., Soares, M. B., Schultz, C. L., & Caldwell, M. W. (2019). A new clevosaurid from the Triassic (Carnian) of Brazil and the rise of sphenodontians in Gondwana. *Scientific Reports*, *9*(1), 11821. https://doi.org/10.1038/s41598-019-48297-9

Jones, M. E. H. (2008). Skull shape and feeding strategy in *Sphenodon* and other Rhynchocephalia (Diapsida: Lepidosauria). *Journal of Morphology*, *269*(8), 945–966. https://doi.org/10.1002/jmor.10634

Jones, M. E. H. (2009). Dentary tooth shape in *Sphenodon* and its fossil relatives (Diapsida: Lepidosauria: Rhynchocephalia). In T. Koppe, G. Meyer, & K. W. Alt (Eds.), *Comparative dental morphology* (Vol. 13, pp. 9–15). Karger Publishers.

Jones, M. E. H., Curtis, N., Fagan, M. J., O'Higgins, P., & Evans, S. E. (2011). Hard tissue anatomy of the cranial joints in *Sphenodon* (Rhynchocephalia): Sutures, kinesis, and skull mechanics. *Palaeontologia Electronica*, *14*(2), 92.

Jones, M. E. H., Curtis, N., O'Higgins, P., Fagan, M., & Evans, S. E. (2009). The head and neck muscles associated with feeding in *Sphenodon* (Reptilia: Lepidosauria: Rhynchocephalia). *Palaeontologia Electronica*, *12*(2), 56.

Kaliontzopoulou, A., Carretero, M., & Llorente, G. (2008). Interspecific and intersexual variation in presacral vertebrae number in *Podarcis bocagei* and *P. carbonelli*. *Amphibia-Reptilia*, *29*(2), 288–292.

Klein, N., & Scheyer, T. M. (2017). Microanatomy and life history in *Palaeopleurosaurus* (Rhynchocephalia: Pleurosauridae) from the Early Jurassic of Germany. *The Science of Nature*, *104*(1), 4. https://doi.org/10.1007/s00114-016-1427-3

Kratochvíl, L., Kubička, L., Vohralík, M., & Starostová, Z. (2018). Variability in vertebral numbers does not contribute to sexual size dimorphism, interspecific variability, or phenotypic plasticity in body size in geckos (Squamata: Gekkota: *Paroedura*). *Journal of Experimental Zoology Part A: Ecological and Integrative Physiology*, *329*(4–5), 185–190. https://doi.org/10.1002/jez.2159

Lee, M. S. Y., Palci, A., Jones, M. E. H., Caldwell, M. W., Holmes, J. D., & Reisz, R. R. (2016). Aquatic adaptations in the four limbs of the snake-like reptile *Tetrapodophis* from the Lower Cretaceous of Brazil. *Cretaceous Research*, *66*, 194–199. https://doi.org/10.1016/j.cretres.2016.06.004

Lemell, P., Natchev, N., Beisser, C. J., & Heiss, E. (2019). Feeding in turtles: Understanding terrestrial and aquatic feeding in a diverse but monophyletic group. In V. Bels & I. Q. Whishaw (Eds.), *Feeding in vertebrates* (pp. 611–642). Springer International Publishing. https://doi.org/10.1007/978-3-030-13739-7_16

Lydekker, R. (1880). *Catalogue of the fossil Reptilia and Amphibia in the British museum* (Vol. 1). British Museum.

Martínez, R. N., Simões, T. R., Sobral, G., & Apesteguía, S. (2021). A Triassic stem lepidosaur illuminates the origin of lizard-like reptiles. *Nature*, *597*(7875), 235–238. https://doi.org/10.1038/s41586-021-03834-3

Mäuser, M. (2015). Die laminierten Plattenkalke von Wattendorf in Oberfranken. In G. Arratia, H.-P. Schultze, H. Tischlinger, & G. Viohl (Eds.), *Solnhofen Ein Fenster in die Jurazeit* (pp. 515–535). Verlag Dr. Friedrich Pfeil.

Meloro, C., & Jones, M. E. H. (2012). Tooth and cranial disparity in the fossil relatives of *Sphenodon* (Rhynchocephalia) dispute the persistent 'living fossil' label. *Journal of Evolutionary Biology*, *25*(11), 2194–2209.

Meyer, R. K., & Schmidt-Kaler, H. (1989). *Paläogeographischer Atlas des süddeutschen Oberjura (Malm)*. Schweizerbart Stuttgart. Retrieved from https://library.wur.nl/WebQuery/titel/521889

Munnecke, A., Westphal, H., & Kölbl-Ebert, M. (2008). Diagenesis of plattenkalk: Examples from the Solnhofen area (upper Jurassic, southern Germany). *Sedimentology*, *55*(6), 1931–1946. https://doi.org/10.1111/j.1365-3091.2008.00975.x

Niebuhr, B., & Pürner, T. (2014). Lithostratigraphie der Weißjura-Gruppe der Frankenalb (außeralpiner Oberjura) und der mittel- bis oberjurassischen Reliktvorkommen zwischen Straubing und Passau (Bayern): Beitrag zur Stratigraphie von Deutschland. *Schriftenreihe der Deutschen Gesellschaft für Geowissenschaften*, *83*, 5–72.

O'Brien, A., Whiteside, D. I., & Marshall, J. E. A. (2018). Anatomical study of two previously undescribed specimens of *Clevosaurus hudsoni* (Lepidosauria: Rhynchocephalia) from Cromhall Quarry, UK, aided by computed tomography, yields additional

information on the skeleton and hitherto undescribed bones. *Zoological Journal of the Linnean Society*, *183*(1), 163–195. https://doi.org/10.1093/zoolinnean/zlx087

Peyer, K., Charbonnier, S., Allain, R., Läng, É., & Vacant, R. (2014). A new look at the Late Jurassic Canjuers conservation Lagerstätte (Tithonian, Var, France). *Comptes Rendus Palevol*, *13*, 403–420. https://doi.org/10.1016/j.crpv.2014.01.007

Rauhut, O. W. M., Heyng, A. M., López-Arbarello, A., & Hecker, A. (2012). A new rhynchocephalian from the Late Jurassic of Germany with a dentition that is unique amongst tetrapods. *PLoS One*, *7*(10), e46839. https://doi.org/10.1371/journal.pone.0046839

Rauhut, O. W. M., & López-Arbarello, A. (2016). Zur Taxonomie der Brückenechse aus dem oberen Jura von Schamhaupten. *Archaeopteryx*, *33*, 1–11.

Rauhut, O. W. M., López-Arbarello, A., Röper, M., & Rothgaenger, M. (2017). Vertebrate fossils from the Kimmeridgian of Brunn: The oldest fauna from the Solnhofen Archipelago (Late Jurassic, Bavaria, Germany). *Zitteliana*, *89*, 305–329.

Reynoso, V.-H. (2000). An unusual aquatic sphenodontian (Reptilia: Diapsida) from the Tlayua Formation (Albian), Central Mexico. *Journal of Paleontology*, *74*(1), 133–148. https://doi.org/10.1666/0022-3360(2000)074<0133:AUASRD>2.0.CO;2

Rieppel, O. (1992). The skull in a hatchling of *Sphenodon punctatus*. *Journal of Herpetology*, *26*(1), 80–84. https://doi.org/10.2307/1565028

Robinson, P. L. (1976). How *Sphenodon* and *Uromastyx* grow their teeth and use them. *Morphology and Biology of Reptiles*, *3*, 43–65.

Romo de Vivar, P. R., Martinelli, A. G., Schmaltz Hsiou, A., & Soares, M. B. (2020). A new rhynchocephalian from the Late Triassic of Southern Brazil enhances eusphenodontian diversity. *Journal of Systematic Palaeontology*, *18*(13), 1103–1126. https://doi.org/10.1080/14772019.2020.1732488

Röper, M. (2005). Field trip B: East Bavarian Plattenkalk-different types of upper Kimmeridgian to lower Tithonian Plattenkalk deposits and facies. *Zitteliana*, *26*, 57–70.

Rothery, T. (2002). Are there juvenile specimens of the aquatic sphenodontid *Pleurosaurus*, and if so, what can they tell us about growth in this group. *Journal of Vertebrate Paleontology*, *22S*, 100A.

Rothery, T. (2005). Juvenile pleurosaurs [Unpublished PhD thesis]. University of McGill.

Russell, A. P., & Bauer, A. M. (2008). The appendicular locomotor apparatus of *Sphenodon* and normal-limbed squamates. In C. Gans, A. Gaunt, and K. Adler, (Eds.), Biology of the Reptilia. Morphology I: *The skull and appendicular locomotor apparatus of Lepidosauria*, (Vol. 21, pp. 1–465).

Schweigert, G. (2007). Ammonite biostratigraphy as a tool for dating Upper Jurassic lithographic limestones from South Germany first results and open questions. *Neues Jahrbuch für Geologie und Paläontologie-Abhandlungen 245*, 117–125. https://doi.org/10.1127/0077-7749/2007/0245-0117

Schweigert, G. (2015). Biostratigraphie der Plattenkalke der südlichen Frankenalb. In G. Arratia, H.-P. Schultze, H. Tischlinger, & G. Viohl (Eds.), *Solnhofen Ein Fenster in die Jurazeit* (pp. 63–66). Verlag Dr. Friedrich Pfeil.

Simões, T. R., Caldwell, M. W., & Pierce, S. E. (2020). Sphenodontian phylogeny and the impact of model choice in Bayesian morphological clock estimates of divergence times and evolutionary rates. *BMC Biology*, *18*(1), 191. https://doi.org/10.1186/s12915-020-00901-5

Simões, T. R., Kinney-Broderick, G., & Pierce, S. E. (2022). An exceptionally preserved *Sphenodon*-like sphenodontian reveals deep time conservation of the tuatara skeleton and ontogeny. *Communications Biology*, *5*(1), 1–19. https://doi.org/10.1038/s42003-022-03144-y

Swinton, W. E. (1939). A new Triassic Rhynchocephalian from Gloucestershire. *Annals and Magazine of Natural History*, *4*(24), 591–594. https://doi.org/10.1080/00222933908655407

Tischlinger, H., & Rauhut, O. W. M. (2015). Schuppenechsen (Lepidosauria). In G. Arratia, H. P. Schultze, H. Tischlinger, & G. Viohl (Eds.), *Solnhofen. Ein Fenster in die Jurazeit* (pp. 431–447). Verlag Dr. Friedrich Pfeil.

Villa, A., Montie, R., Röper, M., Rothgaenger, M., & Rauhut, O. W. M. (2021). *Sphenofontis velserae* gen. et sp. nov., a new rhynchocephalian from the Late Jurassic of Brunn (Solnhofen Archipelago, southern Germany). *PeerJ*, *9*, e11363. https://doi.org/10.7717/peerj.11363

Viohl, G. (2015). Der geologische Rahmen: Die südliche Frankenalb und ihre Entwicklung. In G. Arratia, H.-P. Schultze, H. Tischlinger, & G. Viohl (Eds.), *Solnhofen Ein Fenster in die Jurazeit* (pp. 56–62). Verlag Dr. Friedrich Pfeil.

Von Huene, F. (1952). Revision der Gattung *Pleurosaurus* auf Grund neuer und alter Funde. *Palaeontographica Abteilung*, *101A*, 167–200.

Von Meyer, H. (1831). *Neue fossile Reptilien aus der Ordnung der Saurier* (Vol. 15, pp. 194–195). Nova Acta Academiae Caesareae Leopoldino-Carolinae Germanicae Naturae Curiosorum.

Von Meyer, H. (1847). *Homoeosaurus maximiliani* und *Rhamphorhynchus* (*Pterodactylus*) *longicaudus*: Zwei Fossile Reptilien aus dem Kalkschiefer von Solenhofen. S. Schmerber'schen Buchhandlung.

Von Meyer, H. (Ed.). (1850). Description de l'*Atoposaurus jourdani* et du *Sapheosaurus thiollierei*, reptiles fossiles des calcaires lithographiques du Bugey. *Annales Des Sciences Physiques et Naturelles, d'Agriculture et d'industrie*, *2*, 113–127.

Von Meyer, H. (Ed.). (1854). Acrosaurus frischmanni. *Neues Jahrbuch für Mineralogie, Geologie und Paläontologie, 22*, 47–58.

Wagner, A. (1852). Neu-aufgefundene Saurier-Ueberreste aus den lithographischen Schiefern und dem obern Jurakalke. *Abhandlungen der Bayerischen Akademie der Wissenschaften—Mathematisch-Naturwissenschaftliche Klasse, 6*, 661–710.

Watson, D. M. S. (1914). *Pleurosaurus* and the homologies of the bones of the temporal region of the lizard's skull. *Annals and Magazine of Natural History*, *14*(79), 84–95.

Whiteside, D. I. (1986). The head skeleton of the Rhaetian sphenodontid *Diphydontosaurus avonis* gen. et sp. nov. and the modernizing of a living fossil. *Philosophical Transactions of the Royal Society of London. B, Biological Sciences*, *312*(1156), 379–430. https://doi.org/10.1098/rstb.1986.0014

Williston, S. W. (1925). *The osteology of the reptiles*. Harvard University Press.

How to cite this article: Beccari, V., Villa, A., Jones, M. E. H., Ferreira, G. S., Glaw, F., & Rauhut, O. W. M. (2025). A juvenile pleurosaurid (Lepidosauria: Rhynchocephalia) from the Tithonian of the Mörnsheim Formation, Germany. *The Anatomical Record*, *308*(3), 844–867. https://doi.org/10.1002/ar.25545